3
Airspeed Systems Theory and Calibration

3.1 Introduction

An accurate measurement of airspeed and altitude is necessary for safe flying. This is especially true for flight testing. In addition to the error caused by the airplane's instruments, several other errors are associated with the pitot-static system. This chapter will discuss these errors, the methods for evaluating them, and the requirements for calibration and accuracy as defined in the Federal Aviation Regulations.

3.2 Federal Aviation Regulation Requirements

The FAA and its predecessors have always considered flight instrument accuracy to be important. Aeronautics Bulletin 7-A states: "The 'indicated' airspeed is defined as the speed which would be indicated by a perfect air-speed indicator, namely one which would indicate true air-speed at sea level under standard atmospheric conditions." It further refers the reader to Aeronautics Bulletin 26, section 6(A)(8), for further information on airspeed indicators. Current regulations require accuracies over specified ranges of airspeed and altitude.

3.2.1 Civil Aeronautics Requirements 3.663 Airspeed Indicating System

This regulation requires the airspeed indication system to be so installed as to indicate true airspeed at sea level (calibrated airspeed) under standard conditions within an allowable installation error of no more than $\pm 3\%$ of the calibrated airspeed or 5 statute mph, whichever is greater, between $1.3V_{S1}$ and V_C with the flaps up and at $1.3V_{S1}$ flaps down. The regulation requires the calibration to be made in flight.

3.2.2 Civil Aeronautics Requirement 3.665 Static Air Vent System

This regulation states that airplane speed, the opening and closing of windows, air-flow variation, moisture, or other foreign matter shall not seriously affect the accuracy of instruments that depend upon static pressure.

3.2.3 Federal Aviation Regulation 23.1323 Airspeed Indicating System

FAR 23.1323 is similar to CAR 3.663 except mph have been changed to kn and the ranges for the calibration have changed. In this regulation, the cali-

bration range flaps up is from $1.3V_{S1}$ to V_{MO}/M_{MO} or V_{NE}, whichever is appropriate, and the flaps extended range is from $1.3V_{S1}$ to V_{FE}. The pitot-static system is required to have positive drainage for moisture and must have a heated pitot if IFR certification is sought.

Commuter category airplanes are required to have an additional calibration with the airplane on the ground between $0.8V_{1\min}$ and $1.2V_{1\max}$, which considers the approved ranges of altitude and weight. This calibration must be determined considering an engine failure at $V_{1\min}$. Duplicate systems are also required for commuter category aircraft.

3.2.4 Federal Aviation Regulation 23.1325 Static Pressure System

FAR 23.1325 is considerably more stringent than is CAR 3.665. In addition to requiring the items of CAR 3.665, this regulation contains requirements for drainage, chafing, and distortion of the tubing, and the materials used must be suited for the intended use and protected against corrosion.

In addition, a proof test must be conducted to demonstrate the integrity of the system. These tests are for both pressurized and unpressurized airplanes. For unpressurized airplanes, the test is to evacuate the static system to 1000 ft above the airplane's altitude and determine that the system does not leak down more than 100 ft in 1 min. For pressurized airplanes, the test is to evacuate the system until a pressure differential equal to the maximum pressure differential for which the airplane's cabin is approved is reached. Then, the system should not leak down more than 2% of the altitude equal to the cabin's differential pressure or 100 ft, whichever is greater.

Static pressure ports are also to be designed so that there will not be a significant change in the calibration when the airplane encounters icing.

If a system incorporates a primary and an alternate static source, it must be shown that when either source is selected the other is blocked off and that both can not be blocked off simultaneously.

The static pressure system must be calibrated in flight and the error at sea level on a standard day may not exceed ± 30 ft per 100 kn of airspeed in the speed range between $1.3V_{S0}$ and $1.8V_{S1}$. However the error need not be less than 30 ft.

3.2.5 Advisory Circular 23-8A

Advisory Circular 23-8A provides acceptable methods for calibrating the airspeed system plus precautions for calibration such as static sources located adjacent to the propeller. It also provides data reduction methods in an appendix and an equation to convert airspeed position correction into altimeter position correction.

3.3 Theory of Airspeed Systems

The conventional airspeed indicator is actually a differential pressure gauge calibrated according to the law of frictionless adiabatic flow, with the assumption that the ambient conditions are those of the standard atmosphere at sea level. For subsonic flow the calibration equation is derived from the isentropic

flow relations. Then for subsonic speeds it can be said that:

$$V^2 = 2a^2/\gamma - 1[\{(P_t - P_s/P_s) + 1\}^{\gamma-1/\gamma} - 1] \tag{3.1}$$

For supersonic flow the calibration equation assumes the existence of adiabatic flow with a normal shock located just forward of the total pressure pickup. In this case,

$$P_{t1} - P_s/P_s = \{(\gamma + 1)V^2/2a^2\}^{\gamma/(\gamma-1)}\{\gamma - 1/1 - \gamma + (2\gamma V^2/a)\}^{1/(\gamma-1)} \tag{3.2}$$

where
P_t = free stream total pressure
P_{t1} = total pressure aft of normal shock
P_s = free stream static pressure
γ = specific heat ratio, 1.4 for air
a = free stream sonic speed

Because the airspeed indicator only senses $P_t - P_s$ or $P_{t1} - P_s$ the indicator is calibrated according to the assumption that the sonic velocity has its sea level value of 1117 ft/s, and that the static pressure when it appears alone in the equation also has its sea level value of 2116 psf. By substituting these values into Eq. (3.1) we come up with an equation for calibrated airspeed.

$$V_C = 2497.7[\{(P_t - P_s/2116) + 1\}^{0.2857} - 1]^{.5} \tag{3.3}$$

for subsonic flow with V_C in feet per second, and

$$P_{t1} - P_s = [0.2835V_C^2/\{7 - (1117/V_C)^2\}^{3.5} - 2116] \tag{3.4}$$

for supersonic flow.

Another form of Eq. (3.3) can be obtained by letting

$$q_c = P_t - P_s \tag{3.5}$$

Then by assuming that sonic speed and static pressure have their sea level values we can write:

$$q_C = P_t - P_s = P_{s0}[\{1 + \{(\gamma - 1)/2\}(V_C^2/a_0)\}^{\gamma/(\gamma-1)} - 1] \tag{3.6}$$

If we expand the bracketed quantity by a binomial expansion and retain only the first three terms we have:

$$q_C = P_{s0}\{1 + (\gamma/2)(V_C/a_0)^2 + (\gamma/8)(V_C/a_0)^4 - 1\} \tag{3.7}$$

or

$$q_C = (\gamma P_{s0}/2)(V_C/a_0)^2\{1 + 1/4(V_C/a_0)^2\} \tag{3.8}$$

then if we substitute $\rho_0 = \gamma P_{s0}/a_0^2$ we have:

$$q_C = (\rho_0 V_C^2/2)\{1 + 1/4(V_C/a_0)^2\} \tag{3.9}$$

3.4 Position Error

When we speak of the position error of an airspeed system, we are speaking about the airspeed error caused by the failure of the static and total pressure pickups to sense the actual free stream pressures. This is caused by the location of these pickups on the airframe, hence the name position error. Considerable study has shown that the total pressure source or pitot head is relatively insensitive to inflow angles and will have little error as long as it stays within 20 deg or so of the free stream flow direction. This says that most of the position error is due to location of the static source alone. If we were to plot the static pressure variations around an airplane in flight they would look somewhat like what is shown in Fig. 3.1.

In examining this figure we can see that as the airplane approaches, the pressure increases. In the vicinity of the wing it rapidly changes from maximum positive to maximum negative. About the middle of the aft fuselage it returns to zero and then increases with the oncoming tail. Again, in the vicinity of the horizontal tail it rapidly changes sign. Then somewhere aft of the airplane it returns to free stream value. From this figure we can see that there are very few places on or around the airplane where we can get an accurate reading of the free stream static pressure. This figure also shows why static ports on many airplanes are placed on the aft fuselage. We can also see that in order to do a proper job of flight testing we must have an accurate determination of position error.

To accomplish this by flight test we use several methods. One method is the pitot-static boom located on the nose or the wing tip. To minimize position error wing tip booms should have the static source located a minimum of one chord length ahead of the wing while nose booms should have their static source at least 1.5 fuselage diameters ahead of the fuselage.

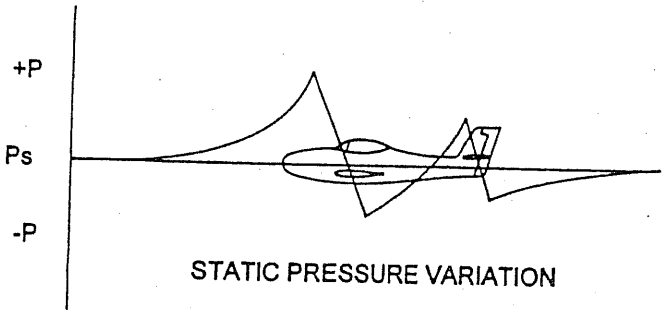

Fig. 3.1 Static pressure change with aircraft passage.

Another method is the airspeed bomb. In this method a bomblike pitot-static source is trailed far enough below and behind the aircraft to sense free stream pressures.

A third method is called the trailing cone method. In this method a trailing cone, with tubing to transmit static pressure, is trailed behind the aircraft at a distance sufficient to obtain free stream static pressure. The distance behind the aircraft of the static pressure ports should be at least 1.5 to 2 aircraft lengths behind the airplane.

All of the methods mentioned have their own set of problems. The fixed pitot-static boom becomes inaccurate at low speed when the angle to the relative wind allows total pressure to enter the static port. A free swiveling boom cures this problem but is not good at high speed due to flutter.

The trailing bomb method is only good for low-speed work since at higher speeds it tends to become unstable.

The trailing cone is good at higher speeds but has a problem with low speed since its weight will cause it to sag, introducing total pressure into the static port.

As you can see, measurement of static pressure during flight test is a sticky problem.

3.5 Lag Errors

Pitot-static systems also suffer from an error called lag error. This particular error shows up on large aircraft where the pitot-static lines are long and on high-performance aircraft where things change rapidly. This error will also show up when either the pitot or static line is longer than the other. To correct and minimize lag errors two steps may be taken. First, attempts should be made to only obtain data during stabilized flight conditions so pressures in the pitot-static system will have time to stabilize. Second, proper attention should be paid to pitot-static system design to insure that both sides have equal volume.

3.6 Altimeter Position Error

Since the altimeter is connected to the static system, it suffers from the same position errors as the airspeed system. The altimeter is calibrated using the equation of balance of the atmosphere:

$$dp = \rho g \, dh \tag{3.10}$$

where
dp = the static pressure change
ρ = air density
g = acceleration due to gravity
dh = change in height

Then for small errors such as position error we can say:

$$\Delta P_s = -\rho g \Delta h p \tag{3.11}$$

where
ΔP_s = the static position error
Δhp = the altimeter position error in feet of pressure altitude

It is worth noting that the altimeter position is a function of altitude since the atmospheric density appears in the equation.

If the airspeed position correction is known, the altimeter position correction can be found using the equation:[7]

$$dH = 0.08865(dV_C)\left\{1 + 0.2\left(\frac{V_C}{661.5}\right)^2\right\}^{2.5}\left(\frac{V_C}{\sigma}\right) \qquad (3.12)$$

where
dH = the altimeter position correction in feet
V_C = the calibrated airspeed in knots
dV_C = the airspeed position correction in knots
σ = the ambient air density ratio

3.7 In-Flight Calibration Methods

Several methods are currently in use for airspeed calibration. They are:

1) speed course method
2) tower fly-by method, or altimeter depression method
3) pace method
4) radar method
5) onboard reference method
6) global positioning system (GPS) method

3.7.1 Speed Course Method

In this method the aircraft is flown over a measured course on the ground at low altitude so an accurate measure of ground speed can be made. The course is flown in both directions and the ground speeds averaged to minimize wind errors. The average ground speed is then compared to the true flight speed and the position error is arrived at. In using this method, attempts are made to fly the course during crosswind conditions and allow the aircraft to drift. This also helps to minimize wind errors. Problems with the method are that it requires a measured course in a remote area and must be flown in very stable air so that airspeed can be maintained accurately. A data reduction sequence for the speed course method is shown in Table 3.1.

3.7.2 Aneroid or Tower Fly-by Method

Since both the airspeed system and altimeter are hooked to the same static system on most aircraft, it is possible to relate altimeter position error directly to airspeed position error using Eq. (3.12).

In this method the aircraft flies at a constant airspeed and altitude by a tower of known height that has an observer and sensitive barometer on top.

Table 3.1 Data reduction for measured speed course method for pitot-static position correction calibration

Step	Item	How to obtain	Units	1	1	2	2	3	3
1	direction of flight	from course layout[a]	deg	090	270	090	270	090	270
2	elapsed time	flight data from stopwatch	min						
3	V_o	flight data	kn	100	100	90	90	80	80
4	H_{Po}	flight data	ft						
5	T_o	flight data	°C						
6	rpm_o	flight data[b]	rpm						
7	$M.\ P._o$	flight data[b]	in. Hg						
8	V_I	instrument calibration	kn						
9	H_{PI}	instrument calibration	ft						
10	T_I	instrument calibration	°C						
11	δ_I	tables or Eq. (1.9)	—						
12	θ_I	273.16 + #10 ÷ 288.16	—						
13	σ	#11 ÷ #12	—						
14	$\sqrt{\sigma}$	$\sqrt{}$#13	—						
15	GS	course distance × 60 ÷ #2	kn						
16	$GS\sqrt{\sigma}$	#15 × #14	kn						
17	Ave. #16	average #16 for opposite headings	kn	—		—		—	
18	Ave. V_I	average #8 for opposite headings	kn	—		—		—	
19	ΔV_{PC}	#17 − #18	kn	—		—		—	

[a] Courses should be laid out so as to be flown cross wind and should be measured in nautical miles.
[b] These flight data only used to help set up the repeat run at the same airspeed.

The observer can determine the aircraft height with respect to the tower using a theodolite. This height may then be compared with the height shown on the aircraft altimeter and the position error determined using Eq. (3.11). This method is almost the exclusive method used by the military and by some aerospace companies. Its problems are:

1) It has speed limitations.
2) It also requires very stable air.
3) It assumes that pitot error is zero.

3.7.3 Pace or Calibrated Aircraft Method

In this method another aircraft is calibrated by one of the above methods and then used as the standard for calibrating the test aircraft. This method has the advantage of safety since the calibration can be done at altitude. It also saves test time since the wait for smooth air at low altitude is not required. Its disadvantage is the requirement to maintain one aircraft in a calibrated state as the standard. The method is performed by the pace or standard aircraft maintaining a steady speed while the test aircraft flies a tight formation on the pace. When there is no relative movement in the formation the test aircraft calls "read data," and both airspeed indicators are read simultaneously. This step is repeated for several speeds through the speed range of the test aircraft.

Correction of data is straightforward. First the pace aircraft's indicated speeds are corrected to calibrated airspeed, then the test aircraft's indicated speeds are corrected for instrument error. The difference between the V_I of the test aircraft and the V_C of the pace aircraft is the ΔV_{PC} for the test aircraft.

3.7.4 Radar Method

The radar method is similar to the speed course method except that the times to traverse the known distance are obtained from the radar. This method has the advantage of being able to be used at altitude and it does not have the speed limitations of other methods. It does, however, require smooth air and low wind conditions. This method is flown in the same manner as the speed course method.

3.7.5 Onboard Reference Method

The onboard reference method consists of using an airspeed bomb or trailing cone as a reference system to calibrate the test aircraft's system. The method is performed by flying the aircraft at a number of speeds throughout its speed range and reading the indications of the test system and the reference system. Data are then reduced in the same manner as the pace method.

The advantages of this method are that it only requires one aircraft and that the reference system may be calibrated on one aircraft and then used on several other aircraft prior to requiring recalibration.

The disadvantages are that the reference system does require calibration and that a special rig or fixture is required on the test aircraft to handle the reference system.

3.7.6 Global Positioning System Method

The global positioning system (GPS) method developed by the author replaces the ground speed obtained from the measured course in the speed course method with the ground speed along the aircraft's heading obtained from GPS ground speed and aircraft track over the Earth. By knowing the GPS ground speed, aircraft track over the ground, and the aircraft heading one can obtain the component of ground speed along the aircraft heading. Like the speed course method, the GPS method uses the ground speed measured along the heading on reciprocal headings to cancel the effects of winds and then follows the speed course procedure for data reduction to determine the pitot-static systems position correction.

The principal advantage of this method is that it can be flown at any altitude as long as the air is smooth. In addition, the aircraft only needs to be stable on altitude and airspeed long enough for the GPS receiver to update—usually a matter of seconds—before data can be read and the opposite heading established.

It should be noted that it is not necessary to have a differential GPS receiver to use this method since its accuracy is quite high with conventional receivers. This is because the ground speed taken from the GPS receiver is the first derivative of the position so a fixed error in the location of the aircraft will not affect the ground speed.

3.8 Temperature Probe Calibration

Since it is customary during the initial stage of flight testing to calibrate all test instruments, we will also discuss calibration of temperature probes. Determination of free air temperature in flight is also subject to correction because of probe design and location. With a well-designed probe the major error is caused by compressing the air passing the probe. If the air passing the probe is brought to a complete stop adiabatically and the probe senses the resulting temperature, then the instrument corrected temperature T_I may be stated by the equation:

$$T_I = T_C + V_T^2/7592 \tag{3.13}$$

where
T_I and T_C are in degrees Kelvin
V_T is in knots
7592 is a constant from the physical properties of air

Since in actuality the air does not come to a complete stop and may exhibit nonadiabatic recovery, a correction factor is added to Eq. (3.13), and the resulting equation is written:

$$T_I = T_C + KV_T^2/7592 \tag{3.14}$$

The correction factor K will vary with installation and probe design from 0.7 to 1.0 but will usually fall between .95 and 1.0. For subsonic speeds K

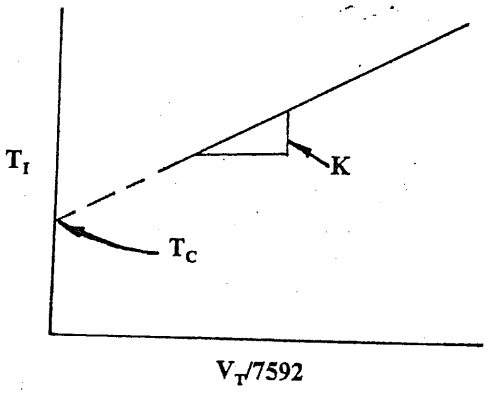

Fig. 3.2 Plot of temperature calibration.

does not vary significantly with Mach number and altitude, but at supersonic speeds temperature rises are much larger and variations may exist.

The constant K may be determined by taking the slope of the plot of T_I vs $V_T^2/7592$ (Fig. 3.2).

The free air temperature T_C may also be determined from this plot by extending the plot to where $V_T^2/7592$ equals zero.

References

[1]Godwin, O. D., Frazier, F. D., and Durnin, R. E., "USAF Performance Flight Test Theory," FTC-TIH 64-2005, AFFTC, USAF Test Pilot School, Edwards AFB, CA, 1965.

[2]Godwin, O. D., Frazier, F. D., and Durnin, R. E., "USAF Performance Flight Test Techniques," FTC-TIH 64-2006, AFFTC, USAF Test Pilot School, Edwards AFB, CA, 1965.

[3]Federal Aviation Administration Order 8110.7, "Engineering Flight Test Guide for Small Airplanes," U.S. Department of Transportation, Federal Aviation Administration, U.S. Government Printing Office, Washington, D.C., 20 June 1972.

[4]Federal Aviation Regulation Part 23, "Airworthiness Standards: Normal, Utility, and Acrobatic Category Airplanes," U.S. Department of Transportation, Federal Aviation Administration, U.S. Government Printing Office, Washington, D.C., June 1974.

[5]Perkins, C. D., Dommasch, D. O., and Durbin, E. J., *AGARD Flight Test Manual, Vol. I—Performance*, Pergamon Press, New York, 1959.

[6]Hamlin, Benson, *Flight Testing*, The MacMillan Company, New York, 1946.

[7]Federal Aviation Administration Advisory Circular No. 23-8A, "Flight Test Guide for Certification of Part 23 Airplanes," U.S. Department of Transportation, Federal Aviation Administration, U.S. Printing Office, Washington, D.C., Feb. 1989.

4
Stall Speed Measurement

4.1 Introduction

The airplane's stalling speed is one of the most important parameters obtained in flight test, since most other criteria are based upon some multiple of stalling speed. Therefore, stalling speed should be determined early in the flight test program. It is the next item to be determined after the pitot-static system has been calibrated. Stalling speed is difficult to determine because the position error is hard to define at high angles of attack and changes rapidly in that region.

One of the difficulties in determining stalling speed is defining when the stall occurs. Airplane designers and aerodynamicists define the stalling speed as the speed at which the maximum lift coefficient, $C_{L\max}$, occurs. However, the various FAA regulations and the military specifications have different definitions. This difference in definition of the stalling speed has led to some controversies during "off-the-shelf" buys of civil certified aircraft by the U.S. military.

4.2 Federal Aviation Administration Requirements

The FAA has several definitions for stalling speed depending upon which certification regulation applies. This also has led to some controversies even within the FAA organization.

4.2.1 Civil Aeronautics Manual 3 Requirements (Ref. 1)

CAR 3.82 Definition of Stalling Speeds states:

(a) V_{S0} denotes the true indicated stalling speed, if obtainable, or the minimum steady flight speed at which the airplane is controllable, in mph, with:

1) engines idling, throttles closed (or no more than sufficient power for zero thrust),
2) propellers in a position normally used for takeoff,
3) landing gear extended,
4) wing flaps in the landing position,
5) cowl flaps closed,
6) center of gravity in the most unfavorable position within the allowable landing range,

7) the weight of the airplane equal to the weight in connection with which V_{S0} is being used as a factor to determine a required performance.

(*b*) V_{S1} denotes the true indicated stalling speed, if obtainable, otherwise the calculated value in mph with:

1) engines idling, throttles closed (or not more than sufficient power for zero thrust);
2) propellers in a position normally used for takeoff, the airplane in all other respects (flaps, landing gear, etc.) in the particular condition existing in the particular test in connection with which V_{S1} is being used;
3) the weight of the airplane equal to the weight in connection with which V_{S1} is being used as a factor to determine a required performance.

(c) These speeds shall be determined by flight tests using the procedure outlined in section 3.120.

Several things should be noted about this regulation. First, the term "true indicated stalling speed" means the calibrated stalling speed. Second, the term "zero thrust" is interpreted by the FAA (then CAA) to permit "zero thrust at a speed not greater than 110% of the stalling speed." The third item that should be noted is that the stalling speed shall be determined by the procedure that is outlined in section 3.120 of CAR 3. This regulation says that: "the elevator control shall be pulled back at a rate such that the airplane speed reduction does not exceed 1 mph per s until a stall is produced as evidenced by an uncontrollable downward pitching motion of the airplane, or until the control reaches the stop." Of all the airplanes upon which the author has measured stalling speed, (50+), the stall has always been defined by when the elevator control reaches the up stop. This condition may be well beyond the maximum lift coefficient if the aircraft has ample elevator power. Even though the airplane may be well beyond the $C_{L\max}$ the elevator is powerful enough to keep the nose from pitching downward uncontrollably until the up stop is reached. If the airplane is elevator power limited the aircraft may reach a steady airspeed without being aerodynamically stalled. In this case the stalling speed is still defined as the speed when the elevator reaches the up stop. It should be noted that the definition of the stalling speed is different than that given in CAR 4b of the CARs and the one given in the military specifications. Fig. 4.1 taken from reference 3 shows these definitions in graphical form.

CAR 3.83 Stalling Speed also addresses the stalling speed. However, in this regulation the maximum value of the stalling speed is addressed. CAR 3.83 says: "V_{S0} at maximum weight shall not exceed 70 mph for 1) single-engine airplanes, and 2) multiengine airplanes which do not have the rate of climb with critical engine inoperative specified in section 3.85(b)." The purpose in this regulation is to lower the stalling speed to a point that in the event of an accident during landing the occupants of the aircraft would have a better chance of survival. Research has shown that the accident rate during landing approach goes up as the square of the approach speed. Therefore, if the stalling speed is low the approach speed will also be low since it is a function of stalling speed.

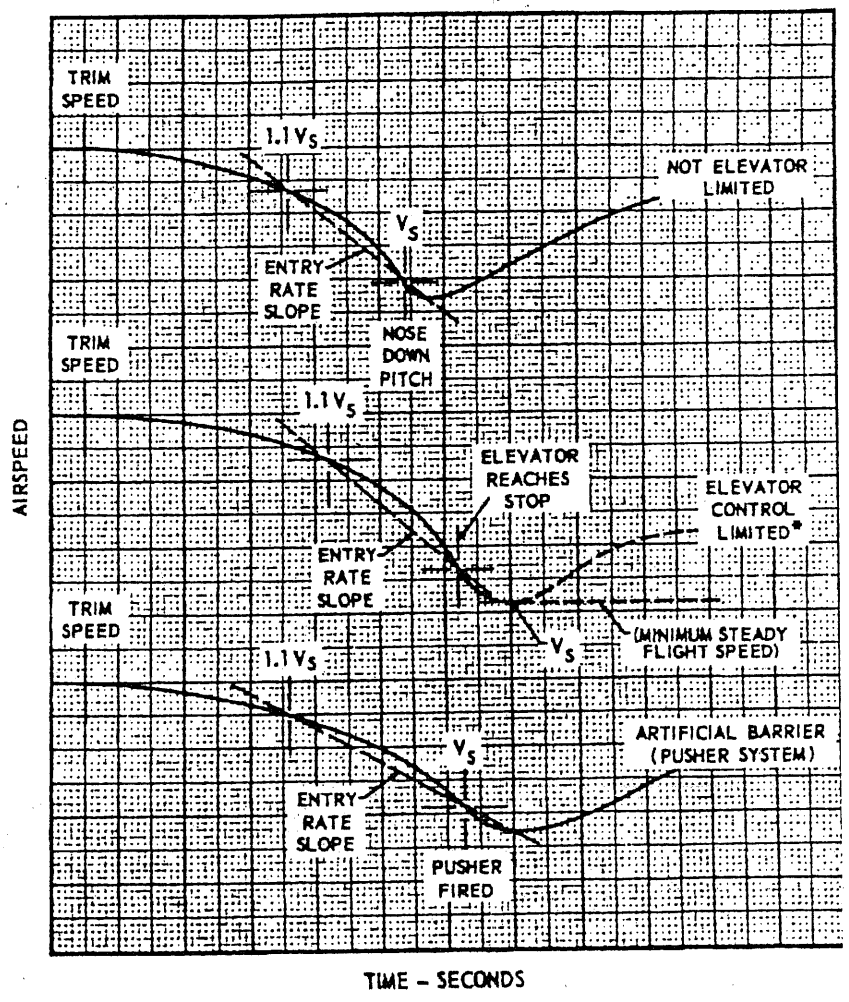

Fig. 4.1 FAA stalling speed definitions.[3]

It is also worthy of note from this regulation that multiengine airplanes that have a stalling speed lower than 70 mph do not have to have a rate of climb when the critical engine is inoperative.

4.2.2 *Federal Aviation Regulation Part 23 (Ref. 2)*

The Federal Aviation Regulations Part 23 reads quite similar to the Civil Aeronautics Regulations. One difference is that the airspeeds have been converted from miles per hour to knots. FAR 23.49 Stalling Speed combines the CAR 3.82 and 3.83 regulations and adds in what had previously been

policy regarding the use of zero thrust at 110% of the stalling speed. FAR 23.49 also refers the reader to FAR 23.201 for test methodology. FAR 23.201 is essentially the same as CAR 3.120 regarding the methodology.

Advisory Circular 23-8A (Ref. 3) has several notes relating to stalling speed. It states that: "the 61 kn (70 mph) stalling speed applies to the maximum takeoff weight for which the airplane is to be certificated." It also points out that most standard airplane pitot-static systems are not acceptable for determining stall speeds and provides some acceptable systems. It also provides acceptable methods for determining zero thrust for reciprocating engine powered airplanes and turbopropeller aircraft. The test crew should consult both the applicable regulations and this advisory circular prior to commencing testing.

4.3 Stall Theory

The stall occurs due to an adverse pressure gradient developing over the upper surface of the wing as the angle of attack is increased causing the flow to separate from the upper surface of the wing. This flow separation is affected by both two-dimensional and three-dimensional effects, in addition to the effects of Reynolds number.

4.3.1 Two-Dimensional Effects

Two-dimensional effects upon the stall and the angle of attack at which it occurs include:

1) Reynolds number
2) wing camber
3) wing thickness
4) size of the leading edge radius
5) surface roughness
6) leading and trailing edge devices such as slots and slats and flaps

4.3.1.1 Reynolds number two-dimensional effects. The larger the Reynolds number, the higher the maximum lift coefficient and the angle of attack where it occurs. Reynolds number has little effect upon the lift curve slope as shown in Fig. 4.2 (Ref. 4).

4.3.1.2 Wing camber effects. Wing camber tends to reduce the angle of attack where stall occurs while increasing the maximum lift coefficient. This effect is similar to that of trailing-edge flaps as shown in Fig. 4.3. Positive camber also moves the angle of zero lift to the left as is also shown in the figure. It is worth noting that for most airfoil families the lift curve slope stays nearly constant with an increase in camber.

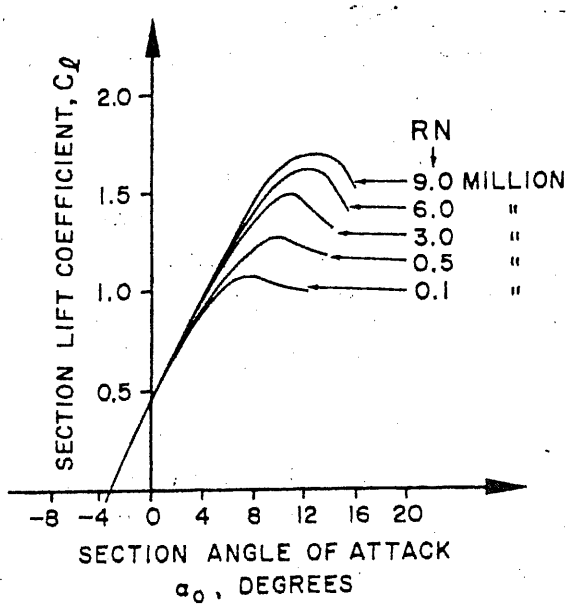

Fig. 4.2 Effect of Reynolds number—NACA 4412 (Ref. 4).

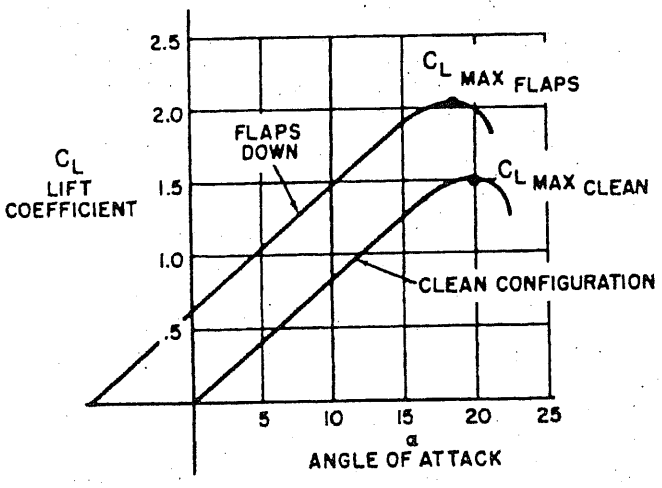

Fig. 4.3 Effects of flaps on the lift curve.[4]

4.3.1.3 Wing thickness effects. Wing thickness has the effect of increasing the maximum lift coefficient and the angle of attack at which it occurs.

4.3.1.4 Leading-edge radius effects. Increasing the size of the leading-edge radius has the effect of increasing the maximum lift coefficient and the angle of attack at which it occurs, thereby delaying the stall.

4.3.1.5 Surface roughness effects. Surface roughness may have varying effects. If the flow over the wing is laminar, an increase in surface roughness will cause the boundary layer to transition to a turbulent boundary layer that contains more energy and will not separate as fast as a laminar boundary layer and the stall will be delayed. However, if the surface roughness is large it may trip the boundary layer causing early separation. Roughness the size of frost or ice will cause the boundary layer to trip resulting in an earlier than normal stall.

4.3.1.6 Leading- and trailing-edge devices effects. Leading- and trailing-edge devices both increase the maximum lift coefficient that an airfoil can produce. However, trailing-edge flaps, of all types, tend to lower the angle of attack at which maximum lift occurs as shown in Fig. 4.3 (Ref. 4). Leading-edge devices, on the other hand, tend to increase the angle of attack where maximum lift occurs. These effects are shown in Fig. 4.4 (Ref. 4).

4.3.2 Three-Dimensional Effects

Three-dimensional effects upon the stall and the angle of attack at which it occurs include:

1) Reynolds number
2) wing planform
3) wing sweep
4) wing aspect ratio
5) effects of aircraft weight
6) effects of c.g. location

4.3.2.1 Reynolds number three-dimensional effects. The Reynolds number role in the three-dimensional effects upon the stall occur as a result of wing planform. If the wing is tapered, the local chord length at the tip is smaller than the chord length at the root, which results in a lower Reynolds number at the tip. As discussed previously, this results in a lower $C_{L\max}$ at the tip and a lower stalling angle of attack. Wing tip stalls are not preferred for stall characteristics since they may produce a roll-off at the stall. Therefore, on many high aspect ratio wings, the chord near the tip is held constant to avoid a reduction in Reynolds number.

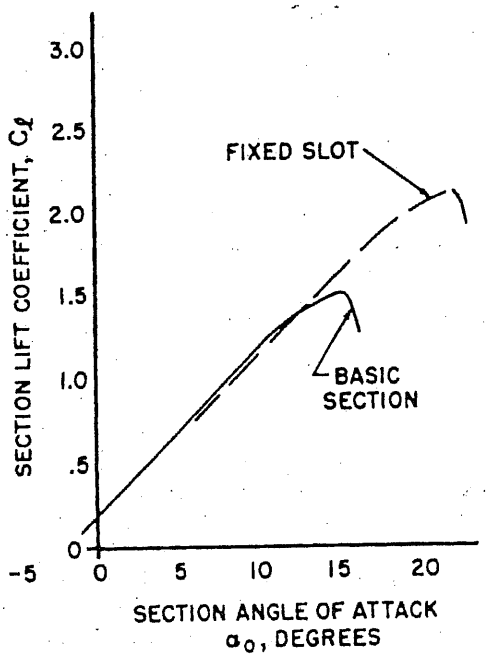

Fig. 4.4 Effects of slots or slats on the lift curve.[4]

4.3.2.2 Wing planform effects. Wing planform has a major effect upon stall. Fig. 4.5 (Ref. 4) shows the stall patterns for several wing planforms. It is desirable from the stall characteristics standpoint to have the wing stall at the root first. From Fig. 4.5, we can see that the rectangular planform is best from the standpoint of stalling at the root first. This good stall behavior is the reason that it is found on many trainer aircraft. However, it is not good from the standpoint of induced drag since it generates large wing tip vortices. The elliptical planform is the best from the standpoint of induced drag, but not good from the standpoint of the stall because it stalls equally along the span. This causes a loss in aileron control early in the stall. Fig. 4.5 also shows the effects of other planforms.

4.3.2.3 Wing sweep effects. Fig. 4.5 also shows the effects of aft sweep. From the figure we can see that aft sweep tends to cause tip stall due to spanwise flow. Forward sweep, on the other hand, uses the spanwise flow to cause the root to stall first, which has been one of the reasons for interest in forward sweep for high-performance aircraft.

4.3.2.4 Effects of aspect ratio. The effects of wing aspect ratio on the stall are shown in Fig. 4.6 (Ref. 4). High aspect ratio wings tend to have higher maximum lift coefficients that occur at lower angles of attack than do low aspect ratio wings. A reduction in aspect ratio can sometimes be used to correct

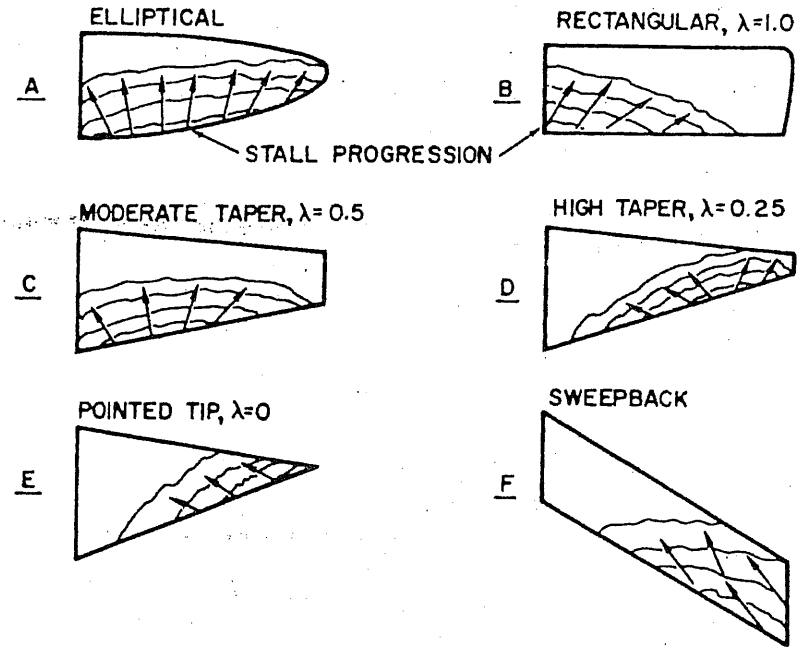

Fig. 4.5 Effects of wing planform on stall patterns.[4]

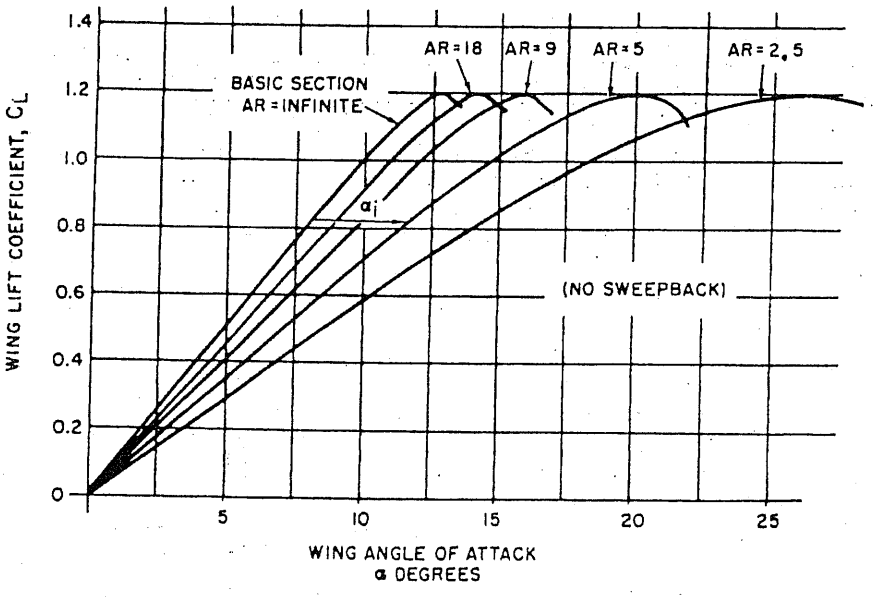

Fig. 4.6 Effects of aspect ratio on three-dimensional wing stall.[4]

problems that occur due to a low stall angle of attack. One such fix is the use of the dorsal fin to correct problems of rudder lock. Although low aspect ratio wings tend to have a higher stall angle of attack, the stall is not as well defined as it is with higher aspect ratios. This can lead to a failure by the pilot to recognize the stall with the resultant development of a very high sink rate. With the introduction of the delta wing F-102 fighter, a number of landing accidents occurred due to this effect.

4.3.2.5 Aircraft weight effects. Aircraft weight has a direct effect upon stalling speed. Stalling speed will increase as weight increases since the maximum lift coefficient is a fixed value.

4.3.2.6 Center of gravity location effects. The location of the aircraft c.g. also has an effect upon stalling speed as well as stall characteristics. Movement of the c.g. aft results in a reduction in the balancing tail down load. This means that the total force the wing must generate is lower, which results in a lower stalling speed. It is for this reason that the FAA regulations require the stalling speed to be measured at the most forward c.g. at maximum TOGW. The c.g. also has an effect upon stalling characteristics. As the c.g. moves aft the longitudinal control becomes more effective allowing the pilot to force the aircraft deeper into the stall prior to reaching the up stop on the elevator. This can result in problems from longitudinal instability (pitch up) to the generation of rolling moments resulting in roll-off.

4.4 Aircraft Loading

As discussed in the previous section, the FAA requires that the stalling speed be measured at the maximum takeoff gross weight at the most forward center of gravity, abbreviated (forward gross). This loading normally results in the highest stalling speed and is the speed published in the "Pilot's Operating Handbook" (POH) or "Airplane Flight Manual" (AFM). Other stalling speeds such as those at aft c.g. at maximum TOGW (aft gross) and the most forward c.g. regardless of weight (forward regardless) may be measured for determining certain flight characteristics, but they will not be used for any performance determination.

4.4.1 Weight and c.g. Tolerances

The weight tolerances as specified by the FAA in both CAM 3 and FAR Part 23 are +5% to −1% of the gross weight at the c.g. where the stalling speed is being determined. It is generally best to overload the aircraft to near the +5% tolerance so that as the flight progresses and fuel is burned the weight does not decrease below the −1% limit.

The c.g. tolerance is ±7% of the total allowable c.g. travel. However, unless it is not possible to do so, it is better to load the aircraft forward of the desired c.g. location particularly if fuel burn off results in aft c.g. movement.

4.5 Safety Considerations

As a rule, measurement of the stalling speed at the forward c.g. is not a hazardous test. However, any time stalls are done for the first time on a new aircraft design care should be taken. Quick release doors should be installed and tested and the aircrew should be attired in helmet, flying suits, parachutes, and jump boots. At forward c.g. it is not necessary to have the aircraft equipped with a spin recovery parachute, but that should be considered before any stall testing is done at c.g. aft of the forward limit.

The altitude selected for initial stall tests is somewhat dependent upon the size of the aircraft. However, in no case should stalls be attempted at altitudes below 5000 ft above ground level (AGL).

Initial stalls should be approached incrementally by recovering at first indication, then at the initial nose pitch, and finally to a complete stall when the elevator hits the up stop. Once it has been determined that the aircraft has reasonable characteristics at this loading, more aggressive testing can be accomplished.

4.6 Flight Test Method

Both CAM 3 and FAR Part 23 provide that stalling speeds are measured at the forward gross loading. In addition, the following other conditions are specified:

1) aircraft trimmed at $1.5V_{S1}$ or $1.5V_{S0}$ depending upon configuration
2) power idle or zero thrust, cowl flaps closed
3) deceleration rate to the stall at 1 kn/s

4.6.1 Trim Airspeed

The trim airspeed for stall speed measurement is 1.5 times the stalling speed in the configuration being tested. One might ask how one knows the value of the stalling speed since it has not been measured. For the first few stalls in a given configuration one can use the calculated stalling speed based upon airfoil data and aircraft takeoff gross weight. Once a more valid test number is obtained from the first few stalls, the test stalling speed can be used and a few stalls repeated at the new trim speed to confirm that stalling speed value.

4.6.2 Power Settings

Both CAM 3 and FAR Part 23 specify either idle power with the propeller set at the maximum rpm setting, or zero thrust. In nearly all cases zero thrust will provide a lower stalling speed, but it is more difficult to obtain since more attention must be paid to power setting during the test. Advisory Circular 23-8A paragraph 23.49(a)(5) provides an acceptable method for determining zero thrust for a propeller-driven aircraft. In essence, the thrust generated by a propeller will be zero when the propeller thrust coefficient, C_T, is zero. Using the propeller manufacturer's coefficient curves one can determine the propeller

advance ratio J at which the thrust coefficient is zero. Knowing this value allows calculation of the propeller rpm necessary for zero thrust by use of the equation:

$$\text{rpm} = 101.27V/JD \tag{4.1}$$

where
rpm = the desired propeller speed setting
V = the airspeed in kn for zero thrust, usually taken at $1.1V_{S1}$
J = the propeller advance ratio at $C_T = 0$
D = the propeller diameter in feet

The test pilot would then assure by adjusting the throttle that this value of rpm was set as the airspeed reached a value 10% in excess of the stalling speed.

4.6.3 Deceleration Rate

The deceleration rate to the stall is 1 kn/s, which should be achieved by the time the speed of $1.1V_{S1}$ is reached during the deceleration. A method for determining this rate is shown in Fig. 4.1 (Ref. 3).

4.6.4 Defining the Stall

The point when the nose pitches uncontrollably is the definition given in CAM 3.120 and FAR 23.201 as the point when the stalling speed is to be measured. Again, it should be stressed that this point occurs for most airplanes of this category when the elevator reaches the up stop. It should also be noted that it must be possible to keep the wings level and sideslip to zero by normal control usage up to this point. Normal control usage means the correct sense of control movement. It does not mean the speed with which the controls are moved. On most airplanes the controls must be moved much faster to correct roll-off after the flow starts to separate.

4.6.5 Statistical Sample

One stall is not adequate to define the stalling speed. At least five stalls should be measured to ensure that a large enough statistical sample is obtained, for a given configuration, to ensure valid data. After each stall has been corrected to standard conditions, the values for the five stalls should be averaged to determine the stalling speed.

4.7 Data Reduction Method

The FAA requires that only a correction for nonstandard weight be made to stall speed data. For small aircraft that is all that is necessary. However, in certain instances it is necessary to correct for deceleration rates that are greater than 1 kn/s or for c.g. positions that are not at forward gross. Therefore, methods for making these corrections are given. However it should be noted that

the FAA does not accept these last two corrections as valid for FAA testing.

4.7.1 Weight Correction

The test weight for each stall accomplished should be determined by knowing the takeoff aircraft loading and the fuel consumed at the time the stall was performed. This can be accomplished by dividing the total fuel consumed during the flight by the total flight time to determine the pounds of fuel used per minute. Then by taking the elapsed time into the flight that the stall occurred, the airplane weight at the time of the stall can be calculated. A second, more accurate and more expensive method to determine the weight at the stall is to use a fuel counter such as is now being installed in many production airplanes and record the pounds of fuel used at the time of the stall.

Once the aircraft weight has been determined, the calibrated stalling speed determined at each data point is corrected for weight using the following equation:

$$V_S = V_{ST}\sqrt{\frac{W_S}{W_T}} \tag{4.2}$$

where

V_S = the weight corrected calibrated stalling speed
V_{ST} = the observed stalling speed corrected for instrument and position error
W_T = the aircraft weight at the stall
W_S = the standard weight, or the weight to which certification is sought; normally the maximum TOGW

Each of the stalls for a specified configuration should be corrected and then averaged to determine the stalling speed to be published.

4.7.2 Deceleration Rate Correction

For most light aircraft testing obtaining the deceleration rate of 1 kn/s by a speed of $1.1V_S$ is not difficult.

4.7.2.1 Correction by the graphical method. Advisory Circular 23-8A provides a graphical method for correcting deceleration rates of greater or less than 1 kn/s. This method may also be used to insure that the stalling speed is measured at a deceleration rate of 1 kn/s. Fig. 4.1 taken from AC 23-8A shows this method and its use.

4.7.2.2 Equation method of correction. Data taken at rates of deceleration greater than 1 kn/s may also be corrected using the following approach:

1) Correct the observed stalling airspeed for instrument and position errors.
2) Apply the nonstandard deceleration correction as follows:

a. Determine the nonsteady flow correction factor, R.

$$R = \frac{V_{Sc}}{(C/2)V} \tag{4.3}$$

where
V_{Sc} = the observed calibrated stalling speed
C = the mean aerodynamic chord
V = the deceleration rate in knots per second

b. Determine the nonstandard rate corrected stalling speed, V_{ST}:

$$V_{ST} = \sqrt{\frac{R+2}{R+1}}(V_{Sc}) \tag{4.4}$$

4.7.3 Center of Gravity Correction

Although not allowed by the FAA regulations, it is possible to make a correction to the stalling speed for an incorrect c.g. position. To accomplish this, one needs to correct the speed for the change in tail down load due to an incorrect c.g. To accomplish this, one must first correct the weight corrected stalling speed to a value of lift coefficient. One then corrects this lift coefficient using the following equation:

$$C_{L_{REF}} = C_{L_{TEST}}\left[1 + \frac{\bar{C}}{l_t}\left(\frac{CG_{REF} - CG_{TEST}}{100}\right)\right] \tag{4.5}$$

where
C_{LREF} = the maximum lift coefficient at the desired c.g.
C_{LTEST} = the maximum lift coefficient at the test c.g.
C = the MAC
l_t = the length of the tail (assumed to be from 1/4 chord of the wing to 1/4 chord of the horizontal tail)

The new lift coefficient is then converted back to stalling speed.

4.7.4 Averaging Corrected Data

Once the corrections have been made to each of the test stalling speeds, they are then averaged to determine the value to be used in pilots' handbooks and for complying with FAA regulations. It is normally a good idea to have at least five stall speeds in a given configuration to average. This insures that the value for the stalling speed that is obtained is a reasonable value and not a scatter point.

References

[1]Civil Aeronautics Manual 3, "Airplane Airworthiness; Normal, Utility, and Acrobatic Categories," U.S. Department of Transportation, Federal Aviation Agency, U.S. Government Printing Office, Washington, D.C., 1959.

[2]Federal Aviation Regulation Part 23, "Airplane Airworthiness; Normal, Utility, and Acrobatic Airplanes," U.S. Department of Transportation, Federal Aviation Administration, U.S. Government Printing Office, Washington, D.C., 1965.

[3]Federal Aviation Administration Advisory Circular No: 23-8A, "Flight Test Guide for Certification of Part 23 Airplanes," U.S. Department of Transportation, Federal Aviation Administration, U.S. Government Printing Office, Washington, D.C., Feb. 1989.

[4]Hurt, H. H., Jr., "Aerodynamics for Naval Aviators," NAVAIR 00-80T-80, U.S. Navy, U.S. Government Printing Office, Washington, D.C., 1960, rev. Jan. 1965.

5
Determination of Engine Power in Flight

5.1 Introduction

In flight testing the determining of engine power is performed for essentially two purposes:

1) To determine the engine power as installed in the airframe.
2) To measure the drag of the airplane with the propulsive system operating.

Because the aircraft's induction, exhaust, and cooling system affect engine power, and engine accessories (such as generators, alternators, or hydraulic pumps) also require power, the manufacturer's tests on a test stand will not give the power of the engine installed in the airframe. In flight testing, then, we must devise methods to measure the actual installed power so we can in turn use this number to define airplane drag. Because the airplane and engine function as a unit we cannot divorce the effects of one on the other. Even though these interaction effects may be small, they can cause data errors when they are ignored. They may also be the cause of poor performance and may be an area to examine when performance does not meet predictions. Some of these interaction effects for propeller-driven airplanes are as follows:

1) effects of cowling shape and blockage on propeller efficiency
2) propeller slipstream effects on airplane drag
3) effects of engine cooling drag on airplane performance
4) effects of engine cooling and fuel distribution on range, cruise, and climb performance
5) effects of engine exhaust thrust on apparent power required
6) effects of induction and exhaust system on power available

Some flight test methods, at least in part, take care of some of these interaction effects and we will discuss these in a later section. The measurement of brake horsepower of the piston engine is fairly straightforward. On the other hand, measurement of thrust horsepower is much more difficult because the interaction effects begin to enter the picture. Also, propeller efficiency charts seldom represent the efficiency of the propeller in its actual operating conditions. As a result most flight test performance data is based on brake horsepower (bhp) rather than on thrust horsepower.

5.2 Power Measurement of an Internal Combustion Engine in Flight

In propeller engine combinations there are several ways of determining engine power. The common methods in use today are: 1) torque meter method; 2) engine power charts; and 3) fuel flow method. Each of these methods has its strengths and weaknesses.

5.2.1 Torque Meter Method

Some flight test organizations believe that engine power is best determined by use of a torque meter attached to the crankshaft to measure torque output. In this method the brake horsepower is given by the equation:

$$BHP_T = KNQ \tag{5.1}$$

where
BHP_T = the test brake horsepower
K = a constant for the torque meter based on dynamometer tests
N = the engine speed (rpm)
Q = the torque meter reading

In some installations the torque is expressed as a function of brake mean effective pressure. In this case Eq. (5.1) can be expressed as:

$$BHP_T = P_bNK \tag{5.2}$$

where
P_b = brake mean effective pressure
K = a constant based on the calibration of P_b and different from the K of Eq. (5.1).

The torque meter method is a good method in the instances where it can be used and where there is a good calibration on the torque meter. It does have some limitations in that most of these devices are large and must be mounted between the propeller and the engine. This moves the propeller farther away from the cowling and may change the propeller efficiency. In addition, the torque meter will change the drag characteristics of the airplane due to its location and considerable care must be exercised in using it when measuring performance. It may be best to use the torque meter to develop an installed power chart by recording manifold pressure (M.P.) and rpm at the same time torque meter readings are taken. These M.P. and rpm values may then be corrected and plotted vs the bhp derived from the torque meter readings and the installed power chart developed. Since in-flight horsepower will vary with airspeed due to ram effects there would be some error depending on how the torque meter affected the overall drag of the airplane. It is, however, still one of the more accurate methods for use in performance testing of propeller-driven airplanes.

5.2.2 Engine Chart Method

In cases where a torque meter cannot be mounted or may be too expensive for the results desired, the engine manufacturer's power charts are an acceptable method. These charts solve for brake horsepower when M.P., rpm, carburetor air temperature, and pressure altitude are known. They are partly derived from actual engine test and partly from theory. They assume that variables other than those mentioned above, which affect engine power, are either constant or vary in a predictable manner. In addition, they assume that fuel flows and fuel distribution to the cylinders are as found on the engine test stand. As you would suspect, all of these items do not exist in an actual installation, so the power charts are not exact. However, for cases where a better method is not available these charts do provide reasonably accurate values of engine power.

The engine performance charts consist of two plots, a sea level chart and an altitude chart. The sea level plot is developed by connecting the engine to a dynamometer with runs being made at constant rpm while varying manifold pressure. The power is measured at each point and a plot such as the left-hand side of Fig. 5.1 (Ref. 3) developed. These lines of constant rpm are straight and converge to a point at zero manifold pressure which is the friction horsepower of the engine.

The altitude side (right-hand side of Fig. 5.1) of the chart converges to zero horsepower at 55,000 ft for normally aspirated engines. It can be developed mathematically from the following equation:

$$BHP_{ALT} = BHP_{SL}\{\sigma - (1 - \sigma)/7.55\} \tag{5.3}$$

or be obtained by flight tests or altitude capable wind tunnels. The test method is preferable, but the equation is based on data collected over many years on different makes of reciprocating engines and is accurate. The altitude side of the chart for turbocharged engines is determined by the engine manufacturer and provided as shown in Fig. 5.2 (Ref. 4). To determine the altitude where the installed engine will no longer develop sea level horsepower (called the critical altitude), one must conduct a flight test discussed later in this chapter.

If the sea level power calibration is available from the engine manufacturer for the test engine, then a power chart may be developed for that specific engine. This provides a more accurate method of power determination for flight testing than using the standard power chart for that type engine. However, if an engine calibration was not obtained for the test engine then the standard manufacturer's chart must be used.

5.2.3 Fuel Flow Method

A third method of determining engine power in flight is the fuel flow method. This method was developed by Textron Lycoming and is based on data accumulated over a period of 30 years. It has been known for many years that the fuel flow going to an engine is a function of the horsepower being developed by that engine or vice versa. In knowing that fact and observing the

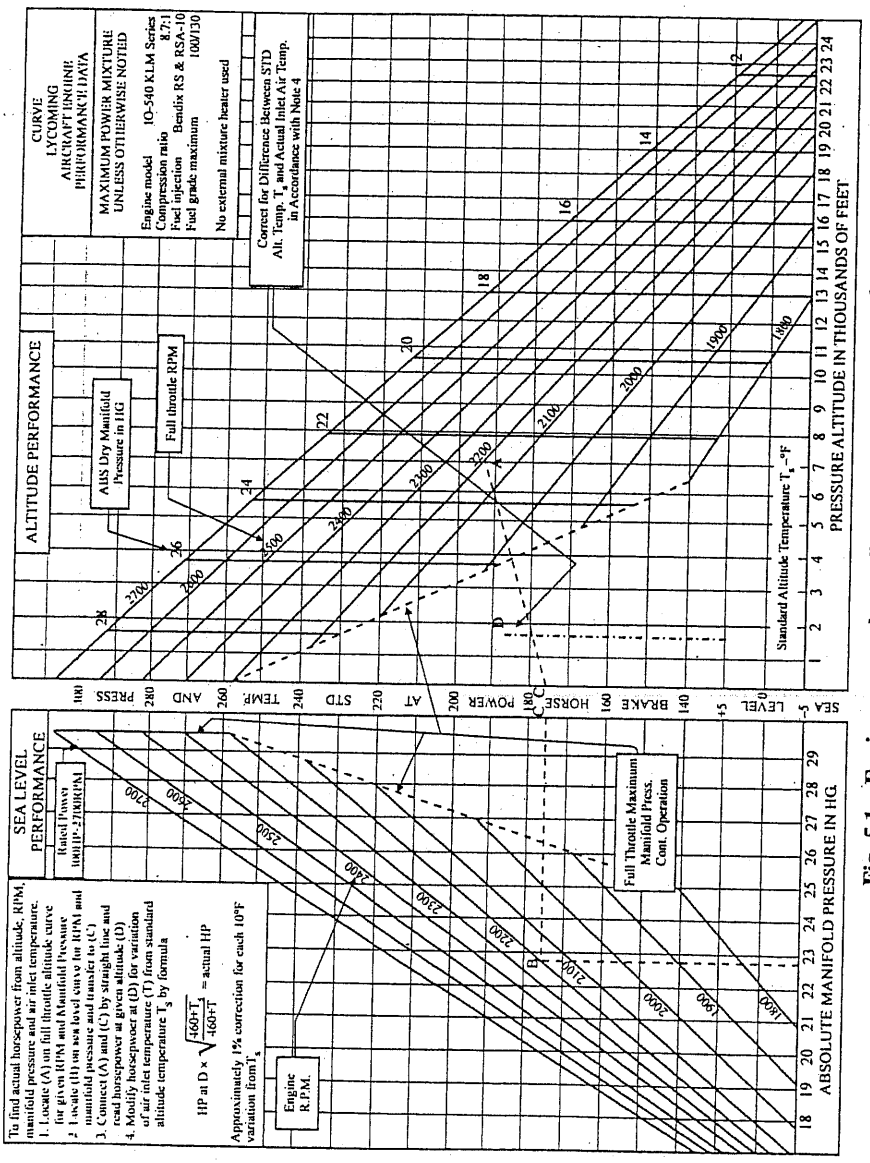

Fig. 5.1 Engine power chart—Lycoming IO-540 engine.[3]

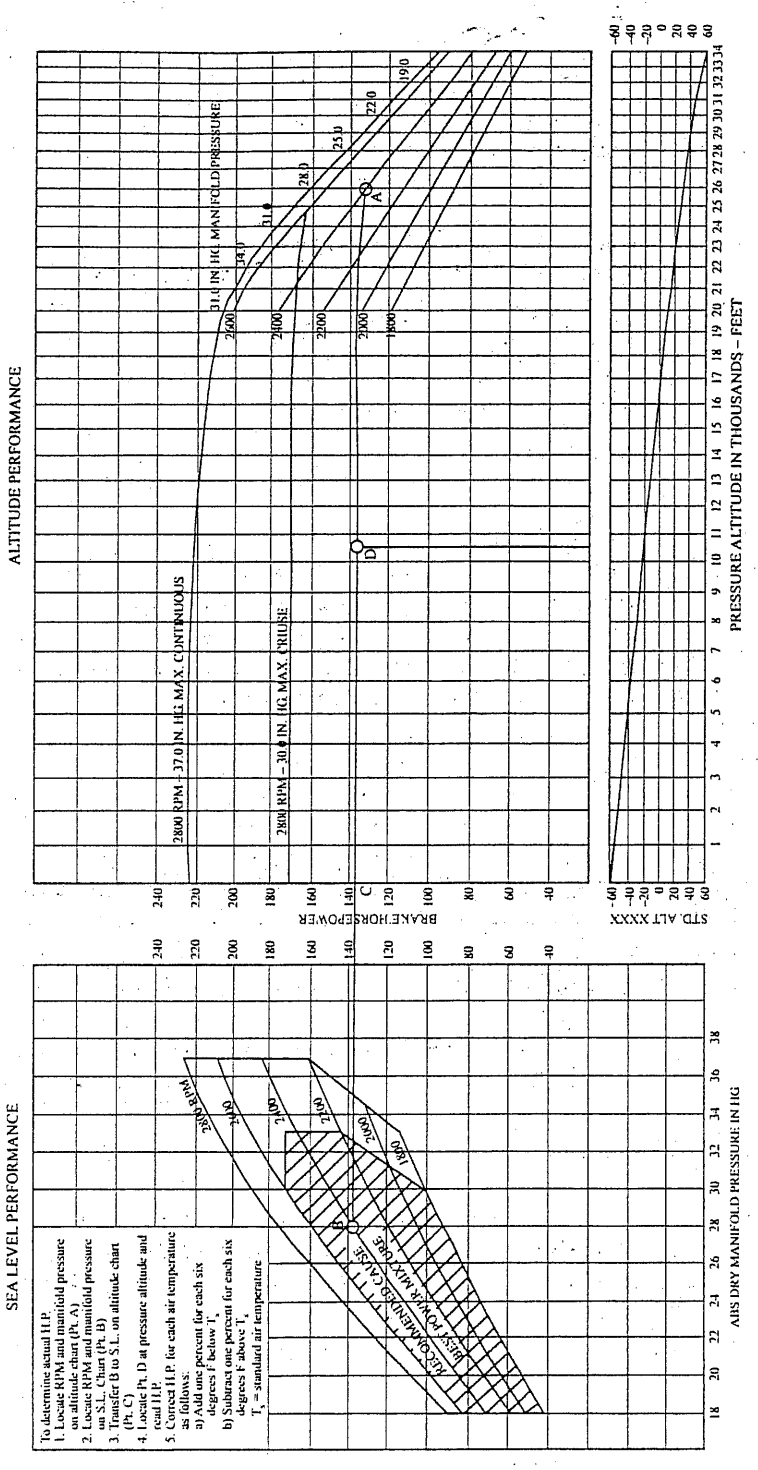

Fig. 5.2 Engine power chart—Continental TSIO-360-C/CB.

data from their engines over a period of time Textron Lycoming reached the following conclusions:

1) At peak exhaust gas temperature (EGT) the engine is developing 96.8% of its best indicated horsepower for the particular throttle setting.
2) At peak EGT the engine has a fuel-air ratio of .0648, which is 84.9% of the best power indicated specific fuel consumption.
3) 100% power occurs between 0.0765 and 0.0840 fuel-air ratio and that for calculations .078 has proved to be an accurate value.
4) The fuel flow varies with the same relationship as the fuel-air ratio.
5) A definite value for indicated specific fuel consumption can be established for each engine as long as the compression ratio is known.

Using the above facts and a series of curves developed on a dynamometer for the engine in question, the actual installed horsepower of the engine can be determined if the fuel flow is accurately measured and the peak EGT carefully established.

Although this method is probably the most accurate method for determining in-flight power, it requires very accurate measurements of fuel flow and EGT which may be beyond the means of some flight test organizations.

5.3 Installed Horsepower Losses and How They Affect Power Measurement

Installed horsepower losses come from four general areas of the engine installation and can be classified as follows:

1) induction system losses
2) exhaust system losses
3) accessory losses
4) improper cooling losses

5.3.1 Induction System Losses

Induction system losses may be further broken down into three items:

1) poor pressure recovery
2) heat rise in the induction system
3) poor fuel distribution due to turbulence in the induction system

Poor pressure recovery in the induction system can be caused by blockage of the inlet, an improper air filter, too many sharp turns in the inlet, or too small an inlet for the engine size. It will normally show up at full throttle as a lower manifold pressure than would be expected for the given conditions.

Heat rise in the induction system will manifest itself as a carburetor air temperature in excess of the free air temperature. It is caused by the induction system being routed through a hot area of the engine compartment, or by leaks of hot air from the carburetor heat or alternate air system.

Poor fuel distribution due to turbulence in the induction system can be caused by any turbulence-producing device in the induction system. If severe enough it may cause rough running of the engine at some power settings. If EGT probes are installed on each cylinder it will show up as EGT for one or more cylinders being much hotter or cooler than the other cylinders.

5.3.2 Exhaust System Losses

Exhaust system losses are caused by poor exhaust system design and by poor selection or design of mufflers. Along with induction system losses, exhaust system losses are two of the largest producers of controllable losses. The exhaust system should be so designed that the pressure pulses from the cylinders do not oppose each other, causing back pressure in the exhaust. The muffler should also be designed with sufficient expansion to prevent excessive back pressure.

5.3.3 Accessory Losses

Accessory losses are fixed losses caused by the power requirements of the various accessories. These losses may be determined by having the engine tested on the dynamometer with and without the accessories. They are variable, however, since the load on such accessories as alternators, hydraulic pumps, or air conditioning compressors may vary. There is little that can be done about these losses other than select the lowest power requirement accessories in design.

5.3.4 Improved Cooling Losses

Improper cooling losses are caused when parts of the engine are not cooled evenly. This can cause increased friction, excessive valve leakage, or piston blow-by losses. To minimize these losses the cooling system should be so designed that the engine and oil temperatures are maintained within the ranges specified by the engine manufacturer. It is essential that differences between individual cylinders and cylinder heads be kept to a minimum.

5.4 Power Corrections

Power corrections may be divided into two general categories: 1) normally aspirated engine corrections; and 2) turbocharged engine corrections.

For normally aspirated engines we can make up to four power corrections:

1) altitude corrections
2) nonstandard temperature corrections
3) humidity corrections
4) full throttle corrections

5.4.1 Altitude Corrections

If we set our altimeter to 29.92 in.Hg and read pressure altitude we do not need to make any correction for altitude. Since this reduces workload it is the route taken by flight test organizations.

5.4.2 Nonstandard Temperature Corrections

Corrections for nonstandard temperature are made because temperature affects air density which affects power. These corrections are made using the following equation:

$$BHP_T = BHP_C\{T_S/(C.A.T._I + 288.16)\}^{0.5} \tag{5.4}$$

where

BHP_T = the corrected test brake horsepower
BHP_C = the brake horsepower obtained from the engine power chart using test conditions of rpm and M.P.
T_S = the standard temperature at the test pressure altitude in degrees Kelvin
$C.A.T._I$ = the instrument corrected carburetor air temperature in degrees Celsius

5.4.3 Humidity Corrections

Since an increase in water vapor in the air causes the air charge entering the engine cylinders to be less dense, it is necessary to make a correction for this where high humidity exists. The correction can be made directly by subtracting the vapor pressure of water, for the given relative humidity, from the instrument corrected observed M.P. If the wet and dry bulb temperatures are read at the flight data point then the vapor pressure of water for that flight data point can be obtained from a psychrometric chart.

5.4.4 Full Throttle Corrections

When operating at full throttle on a normally aspirated engine, or above the critical altitude for a turbocharged engine, we have a condition where any deviation from a standard day results in both a correction for temperature and a correction for manifold pressure. The manifold correction is needed because we cannot increase the manifold pressure due to the throttle being fixed at full open. The full throttle horsepower can then be expressed by the relation:

$$BHP_T = BHP_C + \Delta BHP_{\Delta C.A.T.} + \Delta BHP_{\Delta M.P.} \tag{5.5}$$

The ΔBHP for $\Delta M.P.$ consists of two parts: 1) the $\Delta M.P.$ due to nonstandard temperature; and 2) the $\Delta M.P.$ due to ram effect from increased airspeed. Both of the previously mentioned corrections require considerable instrumentation and, as a result, the full throttle correction is only rarely applied since certain performance methods will account for this correction by simpler means.

For turbocharged engines there are two additional corrections that may need to be considered. They are: 1) power corrections for turbocharger rpm and back pressure variation at a constant manifold pressure; and 2) corrections for determining critical altitude.

5.4.5 Power Corrections for Turbocharger rpm and Back Pressure Variation at Constant Manifold Pressure

On a turbocharged engine, if a given engine rpm and manifold pressure are set, the turbocharger, through its sensing devices, will maintain that power setting by varying its rpm. To vary the turbocharger rpm one must vary the engine back pressure. So, even though the engine power setting remains the same the power output will vary due to the change in engine back pressure and the change in C.A.T. caused by the change in turbo rpm and the free air temperature change.

The power variation due to the change in C.A.T. can be expressed in the same way as Eq. (5.4). The change in power due to change in back pressure has been empirically determined to be one percent increase in power for each 2-in. Hg decrease in back pressure. Then the total correction can be stated as:

$$BHP_T = BHP_C[\{T_S/(C.A.T. + 288.16)\}^{.5} + 0.005(EBP_T - EBP_S)] \qquad (5.6)$$

where
EBP_T = exhaust back pressure for the test conditions
EBP_S = exhaust back pressure for standard day conditions

5.5 Critical Altitude Determination

On a turbocharged engine we reach an altitude where the turbocharger can no longer extract enough energy from the exhaust gases to compress the inlet air enough to maintain the rated manifold pressure. This altitude is defined as the critical altitude. In order to determine this altitude by test we must correct the manifold pressures we observe at each pressure altitude to standard conditions. This is accomplished by the equation:

$$M.P._C = M.P._{OBS}\{T_S/(C.A.T._C + 288.16)\}^{.5} \qquad (5.7)$$

where
$M.P._C$ = standard day manifold pressure
$M.P._{OBS}$ = instrument corrected observed manifold pressure

By plotting the standard day manifold pressure vs pressure altitude the critical altitude may be determined.

References

[1]Herrington, R. M., Maj., Shoemacher, P. E., Bartlett, E. P., and Dunlap, E. W., "USAF Flight Test Engineering Handbook," AFFTCTRN 6273, Air Force Flight Test Center, Edwards AFB, CA, May 1961, rev. June 1964, Jan. 1966.

[2]Perkins, C. D., Dommasch, D. O., and Durbin, E. J., *AGARD Flight Test Manual, Vol. I—Performance*, Pergamon Press, New York, 1959.

[3]Textron Lycoming, "Engine Model Specification," Lycoming IO-540-M Engine, Williamsport, PA, 1967.

[4]Teledyne-Continental Motors, "Owners Handbook," Continental TSIO360-C Engine, Mobile, AL, 1972.

6
Propeller Theory

6.1 Introduction

For certain missions and speed ranges the propeller-driven aircraft is the most efficient. Some examples are:

1) speed range of 0–450 kn
2) certain STOL missions
3) long endurance maritime reconnaissance missions

Recent NASA research has shown it possible to extend the cruise speed of propeller-driven aircraft to 0.8 Mach while maintaining a propeller efficiency in excess of 80%. Therefore for certain applications the propeller will be around indefinitely, and may be reintroduced in such areas as air transport.

6.2 Propeller Theory

There are three theories now used in the design of propellers. They are:

1) momentum theory
2) blade element theory
3) vortex theory

Until recently only the first two theories were in use. This is primarily due to the mathematical complexity of the vortex theory.

Most of today's propellers were designed using blade element theory. The problem for the designer is to find an existing propeller design that can be adapted to their requirements.

Since few propellers have been designed using vortex theory we will limit our discussion to momentum theory and blade element theory. Those interested in vortex theory should read Barnes W. McCormick's *Aerodynamics for V/STOL Flight*, Chapter 4 (Ref. 1).

6.2.1 Momentum Theory

Derived from Newton's second law:

$$F = m(\mathrm{d}V/\mathrm{d}t) \tag{6.1}$$

Assumptions:

1) Propeller does not add rotation to the air.
2) No profile losses.
3) Air is inviscid and incompressible.
4) Propeller has an infinite number of blades.

Since most of these assumptions are unrealistic, this theory is only useful in predicting ideal or maximum propeller efficiencies.

The mass of air passing through propeller (per unit time) is:

$$M = \rho A_1 (V + v) \tag{6.2}$$

where
M = air mass
ρ = air density
A_1 = propeller disc area
V = true airspeed
v = velocity change through propeller

The thrust generated by the propeller is the mass per unit time multiplied times the total change in velocity per unit time through the control volume:

$$F = \rho A_1 (V + v) 2v \tag{6.3}$$

The power input to the propeller is:

$$P_i = F(V + v) \tag{6.4}$$

or the thrust times the velocity change the propeller. The power output by the propeller is:

$$P_o = FV \tag{6.5}$$

The ideal propeller efficiency is defined by:

$$\eta_{Pi} = P_o / P_i = FV / F(V + v) = V / (V + v) \tag{6.6}$$

6.2.2 Blade Element Theory

This theory considers the propeller blade to be a highly twisted wing. Most propellers in use today were designed using this theory. Since this theory considers the propeller to be a highly twisted wing, we will relate, where possible, the propeller parameters to more familiar wing parameters.

r = radius from hub to blade element
V = airplane velocity
β = geometric angle of attack of blade element
γ = reduction in blade angle of attack due to forward velocity

α = actual angle of attack
ω = rotational speed of propeller $\omega = 2\pi n$ where n = rps
u = propeller velocity due to rotation $u = r\omega = 2\pi rn$

$$\tan\gamma = V/u = V/r\omega = V/2\pi rn \tag{6.7}$$

Since β is fixed for a given blade element,

$$\alpha = \beta - \gamma \tag{6.8}$$

For a propeller α is different for each blade element and is not very useful. A better method is to evaluate the propeller at the tip since the twist is fixed. At the tip:

$$\tan\gamma_{tip} = 2V/\omega d \doteq V/\pi nd \tag{6.9}$$

where
d = propeller diameter

The dimension less quantity $V/nd = \pi\tan\gamma_{tip}$ is called the advance ratio J.

$$J = V/nd \tag{6.10}$$

This quantity in propeller theory is used to replace angle of attack in airfoil theory. Using this concept we know that the resultant velocity at a given blade section is proportional to nd, and that the aircraft velocity V is equal to the product of J and nd. We also know that the rotational velocity $u = (2\pi r/d)nd$. We can now arrive at the equation for the thrust generated by the propeller by using the laws of similarity: The propeller diameter as the reference length in determining Reynolds number; The thrust is then the product of the reference area d^2, the dynamic pressure, which corresponds to nd, and a thrust coefficient C_T, which is only a function of J, and the Reynolds number.

$$F = \rho(nd)^2 d^2 C_T = \rho n^2 d^4 C_T \tag{6.11}$$

This equation can be compared to the lift equation of airfoil theory where the constant 1/2 is absorbed into C_T.

In propeller theory we plot C_T vs J like we plot C_L versus α in airfoil theory. In momentum theory we did not consider the drag of the propeller. In blade element theory we do.

The drag goes to make up a part of the moment required to drive the propeller. This moment is the propeller torque Q:

$$Q = \rho n^2 d^5 C_Q \tag{6.12}$$

Where the torque coefficient C_Q is dependent upon J, R_e, and propeller shape.

The power into the propeller is a function of the torque Q and the rate of rotation ω:

$$P_i = \omega Q = 2\pi n Q = \rho n^3 d^5 2\pi C_Q \tag{6.13}$$

or

$$P_i = \rho n^3 d^5 C_p \tag{6.14}$$

where

$$C_P = 2\pi C_Q$$

Since C_Q was dependent upon J, R_e, and propeller shape, so is C_P. The power coefficient is similar to the drag coefficient of airfoil theory and is usually also plotted vs J. The two curves then resemble lift and drag coefficient plots.

To determine efficiency we consider the power out FV divided by the power in P_i:

$$\begin{aligned} \eta_P &= (TV)/P = (\rho n^2 d^4 C_T V)/(\rho n^3 d^5 C_P) \\ &= (C_T/C_P)(V/nd) = (C_T/C_F)(J) \end{aligned} \tag{6.15}$$

Figure 6.1 would be typical of a chart for fixed-pitch propellers. For this kind of propeller there is only one value of J where the efficiency is at a maximum, or since $J = V/nd$ only one flight condition where η_P is at a maximum. So the propeller for the fixed-pitch, propeller-driven airplane is optimized for

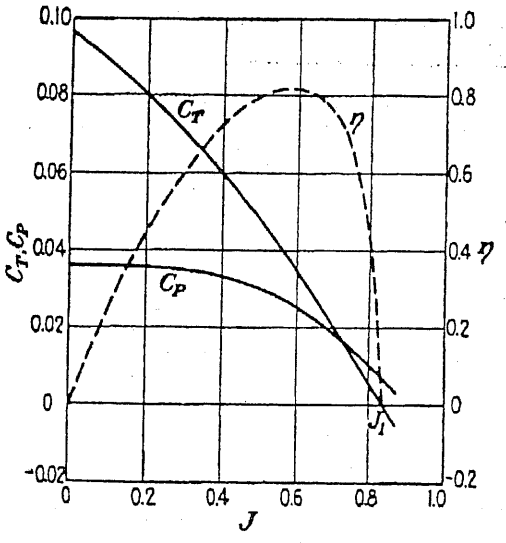

Fig. 6.1 Characteristic curves of a propeller at 15.5 deg blade pitch.[2]

max efficiency in either the climb or cruise condition depending upon its mission.

6.3 Propeller Polar Diagram

For certain flight tests of airplanes it is useful to define the propeller forces to airspeed squared rather than to $(nd)^2$. To do this C_P/J^2 is plotted versus C_T/J^2 such as is shown in Fig. 6.2 for the propeller of Fig. 6.1. From this figure we can see that in this form the propeller data is a straight line which is much easier to use. This curve can be obtained experimentally from flight test data.

6.4 Constant Speed or Controllable Propellers

The efficiency problem with fixed-pitch propellers led to the development of controllable and constant speed propellers. For these propellers there is a family of curves, one set of curves for each blade angle β. This allows us to maintain optimum efficiency over a wide range of J and corresponding flight conditions.

Although a propeller polar such as the one shown in Fig. 6.2 cannot be obtained for a constant speed propeller, Lowry[4] provides a generalized chart for constant speed propellers for light aircraft and Perkins and Hage[5] provide a normalized chart for larger aircraft that was developed by the Boeing Company.

6.5 Activity Factor

The ability of a propeller to absorb power is a function of the blade area as a ratio of the area of the propeller disk. This is expressed as a term called the "activity factor," which represents the integrated power absorption capability

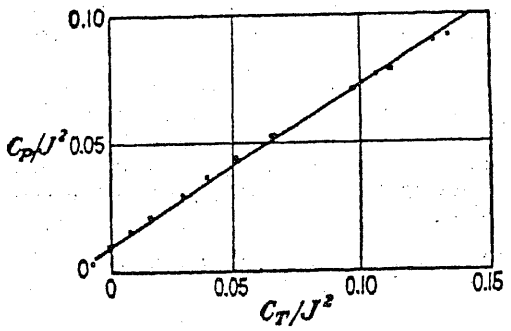

Fig. 6.2 Propeller polar for the propeller of Fig. 6.1 (Ref. 3).

of all the blade elements. The activity factor for a single blade can be found from:

$$A.F. = (100{,}000/16)\int_{.15}^{1.0} (C/D)x^3\,dx \tag{6.16}$$

where $x = (r/R)$ or

$$A.F. = (100{,}000/16)[(C/D)(x^4/4)]_{.15}^{1.0} \tag{6.17}$$

To determine the total activity factor for the propeller one should multiply the activity factor for a single blade by the total number of blades.

6.6 Propeller Noise

The efficiency of a propeller and the noise made by it are also functions of the tip Mach number. In order for a propeller to be efficient and quiet the tip Mach number should be well below 0.9 Mach. In addition, noise may be reduced by increasing the number of blades. However, as the number of blades increase the efficiency of the propeller decreases. A propeller with only one blade is the most efficient propeller.

References

[1]McCormick, Barnes W., *Aerodynamics of V/STOL Flight*, John Wiley and Sons, Inc., New York, 1967.

[2]Weick, Fred E., "Full-Scale Wind-Tunnel Tests with a Series of Propellers of Different Diameters on a Single Fuselage," NACA Technical Report 339, National Advisory Committee on Aeronautics, Langley Field, VA, Jan. 1931.

[3]Von Mises, Richard, *Theory of Flight*, Dover Publications, Inc., New York, 1959.

[4]Lowry, John T., *Performance of Light Aircraft*, AIAA Education Series, AIAA, Reston, VA, 1999.

[5]Perkins, Courtland D., and Hage, Robert E., *Airplane Performance Stability and Control*, John Wiley and Sons, Inc., New York, 1967.

7
Jet Thrust Measurement In Flight

7.1 Introduction

The jet engine presents a separate set of problems for the flight test engineer when attempting to measure jet thrust or power. In many cases it may not be necessary to measure either one of these variables. Instead, the flight data may be referenced to some indication of jet thrust such as "referred rpm", $N/\sqrt{\theta}$, or fuel flow. The pilot does not need to know what thrust the engine is developing in order to operate the airplane as long as the performance information has been referenced to some related variable. However, we always have the problem in flight testing of knowing if our engine is developing the standard thrust for a given rpm or fuel flow. There are also times when we want to determine airplane drag and to do this we need to determine thrust. Before we examine the methods of in-flight thrust measurement, let us review the basic equations for the thrust of a jet engine.

7.2 Basic Theory[1]

A jet engine produces thrust by taking a mass of air in the intake, adding energy, and accelerating it out the tailpipe. The gross thrust developed by this process can be expressed by the equation:

$$F_G = Q_e V_{ex} + A_e(P_e - P_A) \tag{7.1}$$

where
F_G = gross thrust
Q_e = mass flow through tailpipe
V_{ex} = the air mass exit velocity
A_e = the exit area
P_e = the exit static pressure
P_A = ambient static pressure

A measurement of gross thrust does not consider forward motion of the airplane. As the aircraft's speed increases the air entering the intake is compressed prior to entering the aircraft compressor. This compression produces a force that opposes the motion of the airplane. This force is called ram drag and can be expressed as:

$$D_R = QV_T \tag{7.2}$$

where
D_R = ram drag
Q = mass flow rate of air in the inlet
V_T = true airspeed

The net thrust developed by the engine can then be determined by subtracting the ram drag from the gross thrust:

$$F_N = F_G - D_R \tag{7.3}$$

where
F_N = net thrust

If we assume that the mass flow of air in the inlet is the same as the mass flow at the exhaust then we can say:

$$F_N = Q(V_{ex} - V) \tag{7.4}$$

This is probably a reasonable assumption if we consider that the mass of fuel added to the flow is small in comparison to the total mass of air going through the engine.

In measuring the thrust of a jet engine, we must consider conditions at the tailpipe nozzle where the flow may be either subcritical (called unchoked) or sonic (choked). For subcritical or unchoked flow the exit static pressure is equal to the ambient static pressure or:

$$P_e/P_A = 1 \tag{7.5}$$

where
P_e = the static pressure at the nozzle exit
P_A = the ambient static pressure

and the exit temperatures are related by the equation:

$$T_{Tt}/T_e = (P_{Tt}/P_A)^{(\gamma-1)/\gamma} \tag{7.6}$$

where
T_{Tt} = the total temperature in the tailpipe
T_e = the static temperature at the exit
γ = the ratio of specific heats

The exit velocity for the unchoked case is given by the relation:

$$V_{ex} = \{(2\gamma R/\gamma - 1)T_{Tt}[1 - (P_A/P_{Tt})^{(\gamma-1)/\gamma}]\}^{1/2} \tag{7.7}$$

where
R = the gas constant for air

Using the previous assumption that the inlet mass flow rate is equal to the exit mass flow rate, we can express the mass flow rate by the equation:

$$Q = A_e V_{ex}(P_e/RT_e) \tag{7.8}$$

By substitution into Eq. (7.1) and simplifying, the equation for gross thrust of an engine operating in the unchoked condition becomes:

$$F_G/A_e = (2\gamma/\gamma - 1)P_A[(P_{Tt}/P_A)^{\gamma-1/\gamma} - 1] \tag{7.9}$$

If we introduce the pressure ratio into Eq. (7.9) we have:

$$F_G/\delta A_e = (2\gamma/\gamma - 1)P_{SL}[(P_{Tt}/P_A)^{(\gamma-1)/\gamma} - 1] \tag{7.10}$$

where
P_{SL} = the standard atmospheric pressure at sea level

In this equation the term $F_G/\delta A_e$ is only dependent on the ratio of the total tailpipe pressure to the ambient pressure.

A similar set of equations may be obtained for the case of choked flow. The choked flow case follows:

$$P_e/P_{Tt} = (2/\gamma - 1)^{\gamma/(\gamma-1)} \tag{7.11}$$

$$T_e/T_{Tt} = 2/\gamma + 1 \tag{7.12}$$

$$V_{ex} = (\gamma RT_e)^{1/2} \tag{7.13}$$

The mass flow equation is the same as for the unchoked case. Then, by substitution and simplification, the gross thrust equation becomes:

$$F_G/A_e = P_A[(\gamma + 1)(2/\gamma + 1)^{\gamma/(\gamma-1)} \cdot (P_{Tt}/P_A) - 1] \tag{7.14}$$

If we assume that the value for the specific heat ratio γ is approximately 1.33 for flow at elevated temperatures, then Eq. (7.14) can be further simplified to:

$$F_G/\delta A_e = P_{SL}[1.26(P_{Tt}/P_A) - 1] \tag{7.15}$$

For normal nozzles, the flow becomes choked at a pressure ratio of approximately 1.85. Eq. (7.10) would apply to pressure ratios below this number and Eq. (7.15) to those above it. The above equations are based on one-dimensional, isentropic flow.

Since we know that this is not the actual case in a jet engine exhaust, we must add a factor called the thrust coefficient C_f to Eqs. (7.10) and (7.15) to account for the error obtained by making these assumptions. The resulting equations are

$$F_G/\delta A_e = C_f(2\gamma/\gamma - 1)P_{SL}[(P_{Tt}/P_A)^{(\gamma-1)/\gamma} - 1] \tag{7.16}$$

for unchoked flow, and

$$F_G/\delta A_e = C_f P_{SL}[1.26(P_{Ti}/P_A) - 1] \tag{7.17}$$

for choked flow. For the choked flow condition the thrust coefficient is nearly constant varying only between 0.95 and 1.0. For the unchoked case the value of C_f gradually decreases as the pressure ratio decreases.

7.3 Methods of In-Flight Thrust Measurement

There are a number of methods available to the flight test engineer for in-flight thrust measurement on jet power aircraft. However, like power determination on a reciprocating engine-powered aircraft, they all have their weaknesses.

7.3.1 Jet Flow Measurement[1]

One of the more common methods is called the jet flow measurement method. This method works reasonably well on all types of jet engines and can be used as a check on other methods. The method is based on Eqs. (7.16) and (7.17), and gross thrust is determined by measuring the engine pressure ratio (EPR) and solving for gross thrust by use of the equations.

The thrust coefficient C_f is determined by measuring the thrust as a function of EPR during a ground static calibration and plotting C_f as a function of EPR as shown in Fig. 7.1. This ground static calibration should be conducted for each test installation and should be repeated if any engine or airframe component is changed during the test. Since during the ground static calibration it will not be possible to obtain as high a value for EPR as will be obtained in flight, the plot of C_f vs EPR must be extrapolated to the higher values of EPR. It is this extrapolation that is the most likely source of error in the method.

7.3.2 Engine Manufacturer's Data

Another method for in-flight thrust determination is the use of the engine manufacturer's thrust curves and engine calibration data. This is one of the least accurate methods since it does not account for installed thrust losses, and the engine thrust calibration is normally only conducted at sea level. This method would be used only when schedule time or budget restraints did not allow use of a more accurate method.

7.3.3 Wind Tunnel Calibration

If the facilities are available, a calibration of the engine in altitude-capable wind tunnel with the operational inlet and nozzles installed can provide accurate values of both gross and net thrust. This data may then be used for determining thrust in flight. However, care must be taken to insure that the engines used in the flight test and the wind tunnel calibration have the same thrust characteristics. It is preferred to use the same engine for the flight tests as was calibrated in the tunnel, since there may be considerable variation in thrust

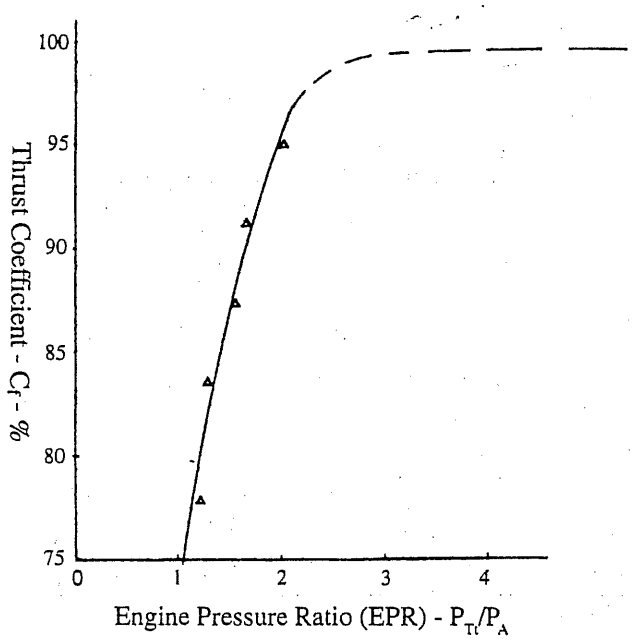

Fig. 7.1 Thrust coefficient vs EPR from static ground calibration.[1]

from engine to engine of the same design. This method costs a large sum of money and is normally only available to those testing military aircraft.

7.3.4 Climb Performance Method[2]

The jet flow method of thrust determination can be criticized for the fact that its accuracy is dependent upon the determination of the thrust coefficient C_f and that C_f values must be extrapolated to EPRs that can be obtained in flight. In addition, this method does not account for the thrust changes due to afterburner operation. There is also a question about the effects of altitude on C_f.

A method developed by the French called the climb performance method removes some of the inaccuracies of the jet flow method and is actually more of an extension of that method than a method that stands alone.

We can assume that the values of C_f obtained during the ground static calibration are accurate at low flight speeds and low altitudes. If we then determine the net thrust by this method in a low altitude climb at best rate-of-climb speed, we can assume it is accurate. If we compare the thrust at this altitude with the thrust obtained at a higher altitude, but with the same values of airspeed and $N/\sqrt{\theta}$, then we can determine if any change with altitude of C_f exists.

By using the same values of climb airspeed and $N/\sqrt{\theta}$ we can assume that the inlet drag is the same for both altitudes. If we also measure the rates of climb at both altitudes we can compare the net thrust at both altitudes by use of the thrust horsepower in excess equation.

$$(F_{NH} - D_H)/(F_{NL} - D_L) = (m_H/m_L)(RC_H/RC_L)(V_H/V_L)^{-1} \tag{7.18}$$

where
m = airplane mass
RC = rate of climb
V = true airspeed
D = airplane drag

subscripts
H = high altitude data
L = low altitude data

By mathematical manipulation we can rewrite Eq. (7.18) as:

$$\begin{aligned} F_{NH}/F_{NL} = {} & (m_H/m_L)(RC_H/RC_L)(V_H/V_L)^{-1} \\ & + \{D_H/D_L + (m_H/m_L)(RC_H/RC_L)(V_H/V_L)^{-1}\}D_L/F_{NL} \end{aligned} \tag{7.19}$$

In a climb the first term of Eq. (7.19) decreases with increasing altitude. The second term only changes slightly. At altitudes where the rate of climb ratio is greater than 0.5 it may be considered of second order and calculated from wind tunnel data.

In addition to providing data on any change in C_f with altitude, Eq. (7.19) may be used to determine the thrust increases due to afterburner operation.

References

[1]Herrington, R. M., Maj., Shoemacher, P. E., Bartlett, E. P., and Dunlap, E. W., "USAF Flight Test Engineering Handbook," AFFTCTRN 6273, Air Force Flight Test Center, Edwards AFB, CA, May 1961, rev. June 1964, Jan. 1966.

[2]Perkins, C. D., Dommasch, D. O., and Durbin, E. J., *AGARD Flight Test Manual, Vol. I—Performance*, Pergamon Press, New York, 1959.

8
Level Flight Performance Theory

8.1 Introduction

Level flight performance may be described as steady state performance. It is a condition where all of the forces acting on the airplane are in balance or:

$$L = W - F \cos \alpha_F \tag{8.1}$$

$$F \cos \alpha_F = D \tag{8.2}$$

where
L = lift
W = airplane weight
F = thrust
α_F = the thrust angle with the horizontal

However, if we assume small angles we can say that thrust is equal to drag and lift is equal to weight.

In level flight performance we are primarily concerned with Eq. (8.2) or thrust F and drag D; however, we shall see that the lift L and weight W of Eq. (8.1) also play a part.

8.2 Thrust Required

Level flight performance is essentially a determination of airplane drag as a function of velocity. Since the thrust must equal the drag it could also be called the thrust required for a given velocity.

The drag of an airplane is composed of two components. They are 1) parasite drag; and 2) induced drag.

The parasite drag is composed of all forms of drag other than the drag due to creating lift which is the induced drag.

Parasite drag can be defined by the equation:

$$D_P = 1/2 C_{DP} \rho V_T^2 S \tag{8.3}$$

where
D_P = parasite drag
C_{DP} = parasite drag coefficient
S = reference area (normally taken as the wing planform area)

From this equation we can see that drag varies as a function of the true airspeed squared.

The induced drag is defined by the equation:

$$D_i = 2L^2/\rho V_T^2 S\pi ARe \tag{8.4}$$

where
D_i = induced drag
S = wing area
AR = aspect ratio
e = Oswald's efficiency factor

This equation shows that the induced drag varies as a function of $1/V_T^2$.

A plot of both parasite and induced drag as a function of airspeed is shown in Fig. 8.1.

If the profile and induced drag are added we arrive at the total drag of the airplane. This plot is also shown in Fig. 8.1. Since thrust must equal drag this curve may also be called the thrust required curve. There are several things that should be known about the thrust required curve for an airplane. First, it is limited on the low-speed end by the stalling speed. Second, the velocity for minimum drag occurs where the parasite and induced drag are equal. This point is the best lift to drag ratio $(L/D)_{max}$ for the airplane. For a jet airplane this is the speed for both best endurance and best glide.

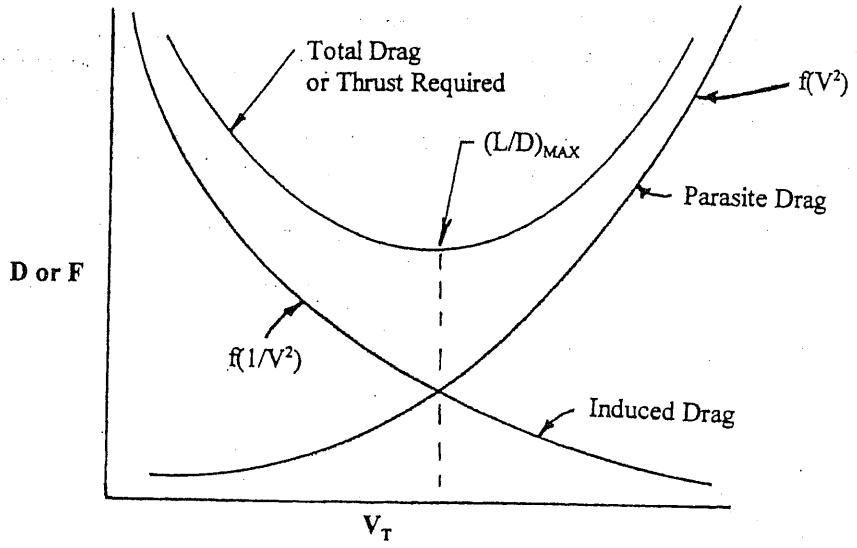

Fig. 8.1 Composition of thrust required curve.

8.3 Effects of Variables on Thrust Required

If one examines Eqs. (8.3) and (8.4) it may be seen that there are two variables other than those already discussed which can affect the thrust required. They are the lift and the air density. If we say that in steady state lift is equal to weight then in actuality the weight becomes the variable.

8.3.1 Effects of Weight

Since the lift, or weight, only appears in the equation for induced drag [Eq. (8.4)], we can say that the weight only affects the induced portion of the thrust required curve. This makes weight effects predominant at the low-speed end of the curve as is shown in Fig. 8.2. An increase in weight increases the thrust required. Fig. 8.2 also shows that the speed for $(L/D)_{max}$ increases as weight increases.

8.3.2 Effects of Air Density

In examining Eqs. (8.3) and (8.4) we can see that a change in density will affect the profile drag directly and the induced drag as a function of $1/\rho$. This has the effect of shifting the thrust required curve to the right as density decreases as is shown in Fig. 8.3. The value of minimum drag or thrust required remains the same, but the true airspeed at which it occurs increases. The effects of density on the thrust required curve can be negated if the thrust plotted against equivalent airspeed V_e. Then only one curve will result. Weight,

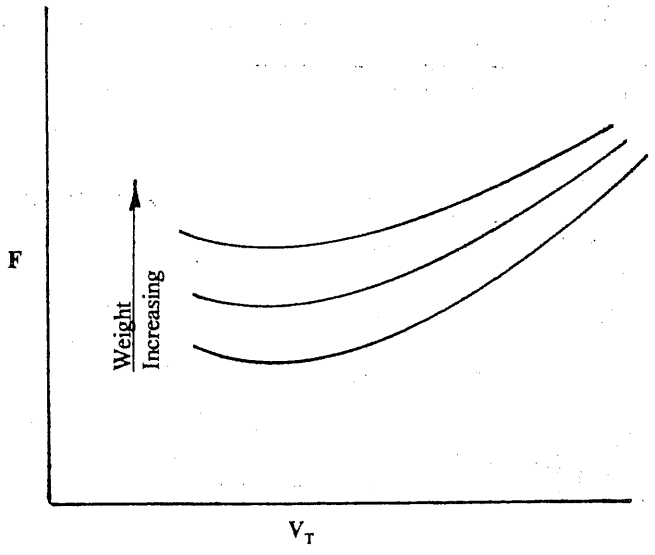

Fig. 8.2 Effects of weight on thrust required.

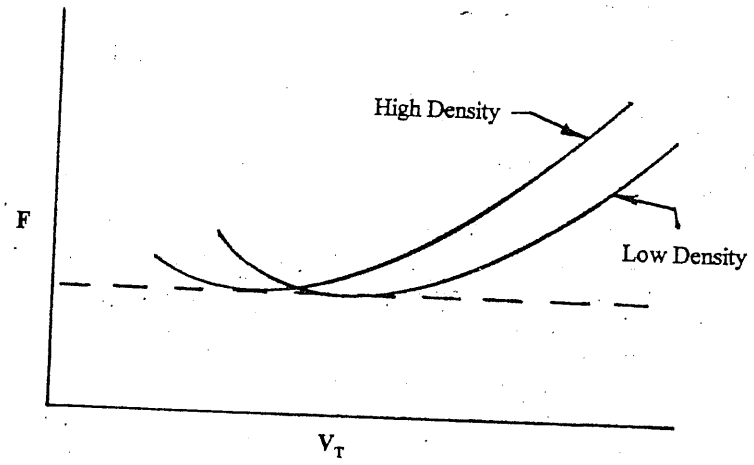

Fig. 8.3 Effects of air density on thrust required.

however, will still cause a shift in the curve even when plotted against V_e as is shown in Fig. 8.4.

8.4 Power Required

In propeller-driven airplanes, it is more convenient to use power required than thrust required. The thrust horsepower required can be stated by the equation:

$$THP_R = F_R V_T / 550 \tag{8.5}$$

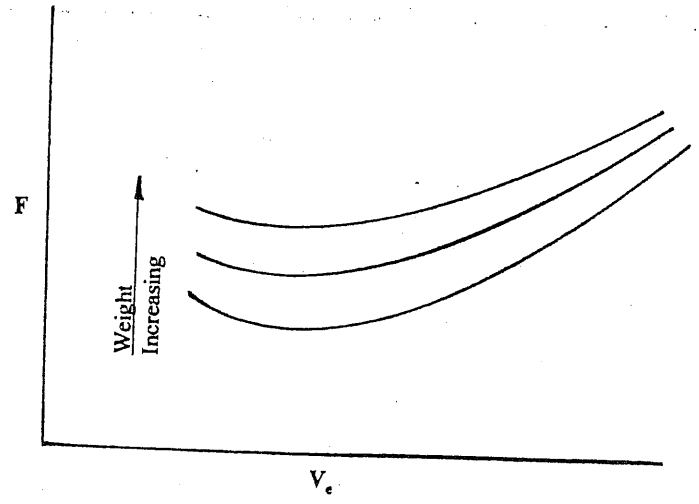

Fig. 8.4 Effects of weight on thrust required when plotted vs equivalent airspeed.

where
THP_R = thrust horsepower required
F_R = thrust required in pounds
V_T = true airspeed in feet per second

If we combine Eqs. (8.3) and (8.4) to obtain the thrust required and substitute that equation into Eq. (8.5) we have:

$$FHP_R = [1/2C_{DP}\rho V_T^3 S + 2L^2/\rho V_T S\pi ARe]/550 \tag{8.6}$$

From this equation we can see that the profile power required varies as the true airspeed cubed, and the induced power required varies as $1/V_T$. This is shown in Fig. 8.5. By adding the profile power required to the induced power required we have the total power required curve also shown in Fig. 8.5. On this curve the minimum drag or best L/D occurs at a higher speed than the speed for lowest FHP_R. The minimum FHP_R is the speed for best endurance on a propeller-driven airplane while the speed for $(L/D)_{max}$ is the best range speed.

8.5 Effects of Variables on the Power Required Curves

Although the same variables affect the power required curve as affect the thrust required curve, they affect them in a different manner.

8.5.1 Effects of Weight

Since weight affects the induced portion of the power required curve its greatest effect occurs at the low-speed end. The general effects of weight on the power required curve are shown in Fig. 8.6.

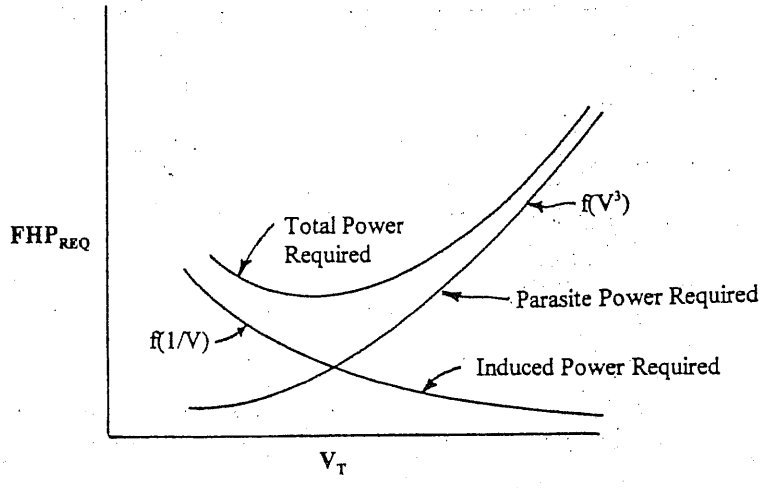

Fig. 8.5 Composition of power required curve.

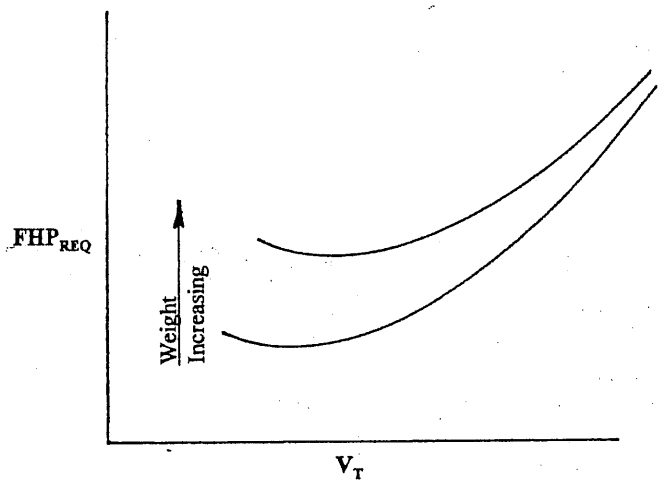

Fig. 8.6 Effects of weight on the power required curve.

In order for the airplane to maintain a given C_L, or angle of attack, when the weight changes one must vary the airspeed. This can be expressed by the relationship:

$$V_2/V_1 = \sqrt{W_2/W_1} \tag{8.7}$$

where
V_1 = the V of a specific C_L and weight, W_1
V_2 = the V for the same C_L but a different weight, W_2

This effect applies to the FHP_R curves and the airspeed will vary by the same relationship on these curves when the weight changes.

8.5.2 Effects of Density

Air density also affects the power required curves. Decreasing density tends to move the curves upward and to the right as shown in Fig. 8.7. The $(L/D)_{max}$ moves up and to the right along a straight line as is shown. If we try to cancel the effects of density by plotting FHP_R vs V_e we find that we stop the movement of the curve to the right with decreasing density, but it still moves upward as is shown in Fig. 8.8. This is because if we substitute the relation $V_T = V_e\sqrt{\sigma}$ into Eq. (8.6) we find that we have:

$$FHP_R = [C_{DP}\rho_0 V_e^3 S/2\sqrt{\sigma} + 2L^2/\rho_0\sqrt{\sigma}V_e S\pi ARe]/550 \tag{8.8}$$

Although we have eliminated the density at altitude from this equation still remaining is the square root of the density ratio σ, so, we still have a density effect.

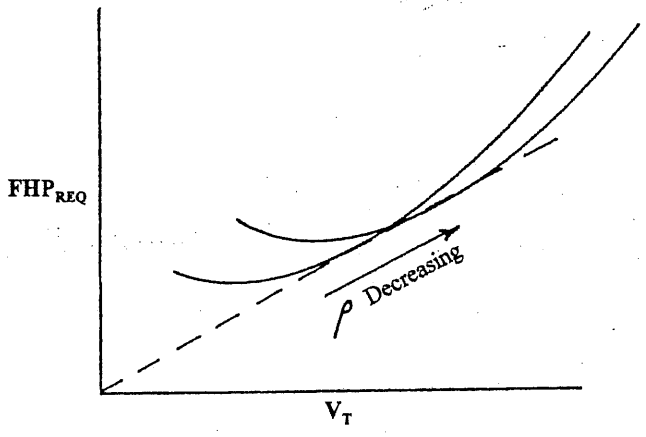

Fig. 8.7 Effects of density on power required.

8.6 Effects of High Mach Number

As an aircraft airspeed approaches Mach 1, the zero lift drag coefficient becomes a variable. (For low Mach numbers it is essentially constant.) This change is caused primarily by the introduction of wave drag.

The result of this change in drag is a rapid increase in the thrust required until Mach 1 is reached. After Mach 1 the drag and the thrust required begins to decrease. This phenomenon is described as the transonic drag rise or transonic thrust pinch.

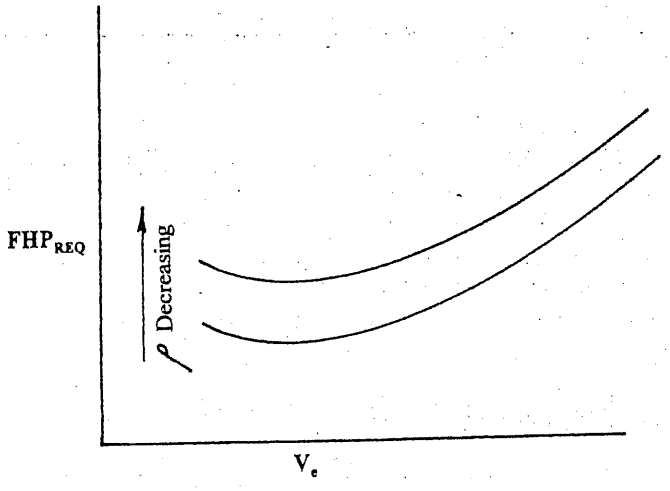

Fig. 8.8 Effects of air density on power required when plotted vs equivalent airspeed.

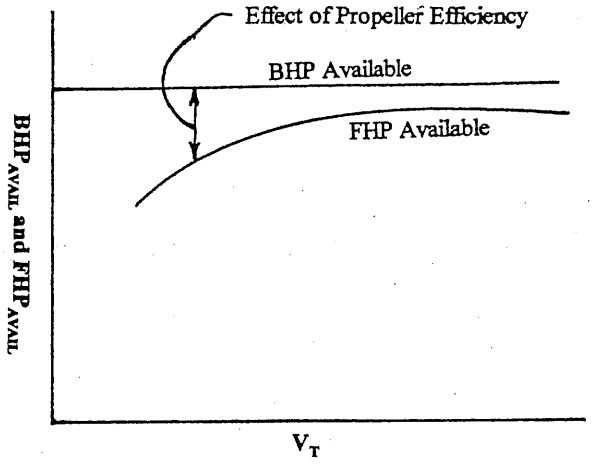

Fig. 8.9 Variation in thrust horsepower available due to propeller efficiency.

8.7 Thrust or Power Available

The thrust or thrust horsepower available is a function of the installed thrust or thrust horsepower of the engine.

Thrust or thrust horsepower will vary with air density; therefore, there will be a different value of thrust or power available for each set of altitude and temperature conditions. Since thrust or thrust horsepower available defines the maximum speed of the airplane, the maximum speed will vary as thrust or power available varies.

On propeller-driven airplanes the propeller efficiency is another variable that will affect the power available. Since propellers are designed to have their maximum efficiency in the normal cruising range of the airplane, the efficiencies will drop on either side of this range. This drop in efficiency occurs on the high-speed end due to tip losses caused by the propeller blades approaching their critical Mach number. On the low-speed end the drop in efficiency is caused by the blades operating at too high an angle of attack. Fig. 8.9 shows a plot of thrust horsepower available and how it varies with propeller efficiency.

References

[1]Godwin, O. D., Frazier, F. D., and Durnin, R. E., "USAF Performance Flight Test Theory," FTC-TIH 64-2005, AFFTC, USAF Test Pilot School, Edwards AFB, CA, 1965.

[2]Godwin, O. D., Frazier, F. D., and Durnin, R. E., "USAF Performance Flight Test Techniques," FTC-TIH 64-2006, AFFTC, USAF Test Pilot School, Edwards AFB, CA, 1965.

[3]Perkins, C. D., Dommasch, D. O., and Durbin, E. J., *AGARD Flight Test Manual, Vol. I—Performance*, Pergamon Press, New York, 1959.

[4]Hamlin, Benson, *Flight Testing*, The MacMillan Co., New York, 1946.